Higher-Order Piezoelectric Plate Theory Derived from a Three-Dimensional Variational Principle

R. C. Batra[*] and S. Vidoli[†]

Virginia Polytechnic Institute and State University, Blacksburg, Virginia 24061

A three-dimensional mixed variational principle is used to derive a Kth-order two-dimensional linear theory for an anisotropic homogeneous piezoelectric (PZT) plate. The mechanical displacements, the electric potential, the in-plane components of the stress tensor, and the in-plane components of the electric displacement are expressed as a finite series of order K in the thickness coordinate by taking Legendre polynomials as the basis functions. However, the transverse shear stress, the transverse normal stress, and the transverse electric displacement are expressed as a finite series of order $(K + 2)$ in the thickness coordinate. The formulation accounts for the double forces without moments that may change the thickness of the plate. Results obtained by using the plate theory are given for the bending of a cantilever thick plate loaded on the top and the bottom surfaces by uniformly distributed 1) normal tractions and 2) tangential tractions. Results are also computed for the bending of a cantilever thick PZT beam loaded by 1) a uniformly distributed charge density on the top and the bottom surfaces and 2) equal and opposite normal tractions distributed uniformly only on a part of the beam. The seventh-order plate theory captures well the boundary-layer effects near the clamped and the free edges and adjacent to the top and the bottom surfaces of a thick orthotropic cantilever beam with the span to the thickness ratio of two. Also, through-the-thickness variation of the transverse shear and the transverse normal stresses agree well with those computed from the analytical solution of the three-dimensional elasticity equations. The governing partial differential equations are second order, so that Lagrange basis functions can be used to solve the problem by the finite element method.

I. Introduction

BECAUSE of the enormous amount of literature on the theory of plates, it is nearly impossible to cite and review all of the papers. The literature on higher-order theories of piezoelectric (PZT) plates has recently been summarized by Wang and Yang.[1] Various attempts to systematically derive plate and rod theories have been reviewed by Koiter and Simmonds,[2] Naghdi,[3] Antman,[4] and Leissa,[5,6] among others. Naghdi[3] and Antman[4] have also discussed Cosserat's[7] direct theories of plates and rods, wherein the plate is modeled as a two-dimensional surface with a number of directors attached to each point; these directors are not tangent to the surface, and their deformation accounts for the transverse deformations of the plate.

Teresi and Tiero[8] deduced plate theories by finding stationary points in suitable subspaces of the functional spaces in which the potential energy, the complementary energy, and the Hellinger–Prange–Reissner functionals are defined. For an isotropic plate, these methods were shown to give different values of the flexural and the shear rigidities. Soldatos and Watson[9] have proposed an improved higher-order plate theory that incorporates the through-the-thickness shape functions obtained from the exact solution of the corresponding simply supported plate. The boundary conditions at the edges are applied in an average sense as in other plate theories. Higher-order plate theories have also been formulated by Mindlin and Medick,[10] Vlasov,[11] Lo et al.,[12] Kant,[13] Reddy,[14] Hanna and Leissa,[15] Lee and Yu,[16] and Lee et al.[17]; this list is by no means complete. Exceptions to the usual expansions of the mechanical displacements and the electric potential as a power series in the thickness coordinate are the works of Soldatos and Watson,[9] Mindlin and Medick,[10] and Lee et al.[17] Soldatos and Watson[9] use exponential functions, Mindlin and Medick[10] use Legendre polynomials, and

Lee et al.[17] use trigonometric functions. Higher-order plate theories derived by employing different basis functions are not necessarily equivalent because the first-order theory of Lee et al.[17] involves $\cos(\pi/2)(1 - z)$, where $z\,(-1 \leq z \leq 1)$ is the normalized thickness coordinate, and the first-order theory of Mindlin and Medick[10] expresses mechanical displacements and electric potential as an affine function of z.

Vidoli and Batra[18] presumed an affine variation in the thickness direction of the three components of the mechanical displacement, the electric potential, the in-plane components of the stress tensor, and the in-plane components of the electric displacement, cubic variation in the thickness direction of the transverse shear stresses, and quadratic variation in the thickness direction of the transverse normal stress and of the transverse component of the electric displacement. They employed a mixed variational principle of Yang and Batra[19] to derive the balance laws, boundary conditions, and constitutive relations for a PZT plate. The theory accounts for the normal and the tangential tractions and the surface charge density prescribed on the top and the bottom surfaces of the plate. The three-dimensional analytical solutions of Vel and Batra[20] for thick laminated structures with PZT patches either embedded in or bonded to their surfaces reveal that the variation of the mechanical displacements and the electric potential is nonaffine. Here we develop a Kth-order theory for an anisotropic PZT plate in which all three components of the mechanical displacement and the electric potential are expanded in the transverse coordinate z, and terms up to z^K are kept in these expansions. The plate theory derived by Vidoli and Batra[18] follows from the one presented herein by setting $K = 1$. Their first-order shear and normal deformable plate theory cannot predict boundary layers near the clamped and free edges and adjacent to the top and bottom surfaces of the plate; however, the present higher-order plate theory can predict these effects. The present Kth-order plate theory differs from those derived by Mindlin and Medick,[10] Lee and Yu,[16] and Lee et al.,[17] at least in the following respects. Whereas we express the transverse shear stresses, the transverse normal stress, and the transverse electric displacement as polynomials of degree $(K + 2)$ in z, with the remaining variables expressed as polynomials of degree K in z, they use basis functions of the same order to expand all of the variables. Surface tractions and surface charges prescribed on the top and the bottom surfaces of the plate also appear explicitly in the present two-dimensional constitutive relations. Thus, natural

*Clifton C. Garvin Professor, Department of Engineering Science and Mechanics, M/C. 0219.

†Postdoctoral Research Associate, Department of Engineering Science and Mechanics, M/C. 0219.

boundary conditions on these surfaces are exactly satisfied. In other plate theories, surface tractions and surface charges acting on the top and the bottom surfaces appear only in the two-dimensional balance of linear momentum. Lee et al.[17] use the principle of virtual work to derive boundary condtions [Eqs. $(21)_1$ of Ref. 17] on the top and the bottom surfaces of the plate. We note that in the present theory the transverse normal and the transverse shear stresses are computed from the displacement fields obtained by solving the two-dimensional equations of the plate theory rather than by integrating a posteriori the three-dimensional equations of elasticity.

It is shown that the results predicted by a seventh-order plate theory compare very well with the analytical solution for the cylindrical bending of a thick cantilever plate with the span to the thickness ratio of two and loaded on its top and bottom surfaces by a uniformly distributed load. Note that a plate with an aspect ratio of two is a three-dimensional body. Thus, it is not surprising that a significantly higher-order plate theory is needed to compute good results. The proposed plate theory predicts boundary-layer effects near the top and the bottom surfaces of the plate where loads are specified. The through-the-thickness distributions of the transverse shear stress and the transverse normal stress near the clamped and the free edges compare well with the analytical solution of Vel and Batra[20] for the same problem. We also compute, for different aspect ratios (span/thickness) of the plate, contributions to the total strain energy of the plate made by the bending, the transverse shear, and the transverse extensional modes of deformation. It is found that, even for an aspect ratio of 20, the strain energy due to the transverse shear deformations equals about 10% of the total energy of deformation of the plate. For a plate with an aspect ratio of two, the total strain energies of bending, transverse shear, and transverse extensional deformations change rapidly when K is increased from 1 to 4, but very slowly for $4 < K \leq 6$, and are virtually unchanged when K is increased from 6 to 7. The theory is also used to study the cylindrical bending deformations of a PZT thick cantilever plate loaded on the top and the bottom surfaces by a uniformly distributed charge and by double forces without moments.

II.   Formulation of the Problem

We use rectangular Cartesian coordinates to describe infinitesimal static electromechanical deformations of a linear PZT plate with the x_3 axis perpendicular to the top surface $\mathcal{S}^+$ and the bottom surface $\mathcal{S}^-$ of the plate and the origin on its midplane $\mathcal{S}$. We assume that in the reference configuration the length scale has been normalized by thickness/two so that $x_3 = +1$ and -1 at points on $\mathcal{S}^+$ and $\mathcal{S}^-$, respectively. Thus, in the reference configuration the plate occupies the region $\mathcal{C} = \mathcal{S} \times I$, where $I = [-1, 1]$, $\mathcal{S}^+ = \mathcal{S} \times \{+1\}$, and $\mathcal{S}^- = \mathcal{S} \times \{-1\}$. The boundary $\partial\mathcal{C}$ of the plate is given by

$$\partial\mathcal{C} = (\partial\mathcal{S} \times I) \cup (\mathcal{S}^+ \cup \mathcal{S}^-) = \mathcal{M} \cup \mathcal{U}_\mathcal{B} \qquad (1)$$

where $\partial\mathcal{S}$ is the periphery of $\mathcal{S}$, $\mathcal{M}$ is the mantle of $\mathcal{C}$ or the edges of the plate, and $\mathcal{U}_\mathcal{B}$ is the union of the upper and the lower surfaces of the plate. In a mechanical problem, surface tractions are generally prescribed on $\mathcal{U}_\mathcal{B}$ and surface tractions and/or mechanical displacements on $\mathcal{M}$. In the electromechanical problem being studied here, the analogous situation will be the specification of surface tractions t and the electric charge density χ on $\mathcal{U}_\mathcal{B}$. However, at a point of $\mathcal{M}$, either t, or the mechanical displacement u, or their linearly independent combination, and χ, or the electric potential φ, are prescribed. Problems in which φ instead of χ is prescribed on $\mathcal{U}_\mathcal{B}$ require a small modification in the derivation of the equations for the plate.

The equilibrium equations, the boundary conditions, and the constitutive relations for a linear PZT body are obtained by finding a saddle point of the following mixed functional of Yang and Batra[19]:

$$\mathfrak{H}(u, S, \varphi, D) = \int_\mathcal{C} b \cdot u + \int_{\partial_a\mathcal{C}} Sn \cdot (u - \bar{u}) + \int_{\partial_b\mathcal{C}} t \cdot u$$

$$- \int_\mathcal{C} S \cdot E(u) + \int_\mathcal{C} q\varphi + \int_{\partial_\alpha\mathcal{C}} D \cdot n(\varphi - \bar{\varphi}) + \int_{\partial_\beta\mathcal{C}} \chi\varphi$$

$$- \int_\mathcal{C} D \cdot W(\varphi) + \frac{1}{2}\int_\mathcal{C} [S \cdot (\mathbb{F}S + \mathbb{M}D) + D \cdot (\mathbb{N}D - \mathbb{M}^\top S)] \quad (2)$$

Here b is the body force per unit volume, S is the stress tensor, n is an outward unit normal to $\partial\mathcal{C}$ that lies in the surface $\mathcal{S}$, $\bar{u}$ is the displacements prescribed on the part $\partial_a\mathcal{C}$ of the boundary $\partial\mathcal{C}$ of $\mathcal{C}$, $E(u) = \text{sym grad}\, u = [\text{grad}\, u + (\text{grad}\, u)^T]/2$ is the strain tensor for infinitesimal deformations, $(\text{grad}\, u)_{ij} = \partial u_i / \partial x_j$, $W(\varphi) = \text{grad}\, \varphi$ is the electric field, φ is the electric potential, q is the density of distributed charges, D is the electric displacement, χ is the density of surface charges, $\bar{\varphi}$ is the prescribed electric potential on the part $\partial_\alpha\mathcal{C}$ of the boundary of $\mathcal{C}$, $\mathbb{F}$ is the fourth-order compliance tensor, $\mathbb{M}$ is the third-order tensor describing the PZT coupling, $\mathbb{N}$ is the second-order dielectric permittivity tensor, and

$$E = \mathbb{F}S + \mathbb{M}D, \qquad W = \mathbb{N}D - \mathbb{M}^T S \qquad (3)$$

are the constitutive relations for an anisotropic linear PZT body. Here E and S are written as six-dimensional vectors and W and D as three-dimensional vectors. Thus $\mathbb{F}$, $\mathbb{M}$, and $\mathbb{N}$ are 6×6, 6×3, and 3×3 matrices, respectively. We note that electric quantities analogous to mechanical quantities b, S, t, u, and E are q, D, χ, φ, and W, respectively. In Eq. (2), $b \cdot u$ denotes the inner product between vectors b and u, and the inner product $A \cdot B$ between second-order tensors A and B is defined as $\text{tr}(AB^T)$, where $\text{tr}(A)$ equals the sum of the diagonal elements of A. For brevity, the variable of integration in Eq. (2) has been omitted; however, it should be clear from the specified domain of integration. Furthermore,

$$\partial_a\mathcal{C} \cup \partial_b\mathcal{C} = \partial\mathcal{C}, \qquad \partial_a\mathcal{C} \cap \partial_b\mathcal{C} = \emptyset$$

$$\partial_\alpha\mathcal{C} \cup \partial_\beta\mathcal{C} = \partial\mathcal{C}, \qquad \partial_\alpha\mathcal{C} \cap \partial_\beta\mathcal{C} = \emptyset \qquad (4)$$

The variation of the functional $\mathfrak{H}$ with respect to the kinematical fields u and φ yields the equations of equilibrium and the natural boundary conditions. The variation of $\mathfrak{H}$ with respect to the kinetic fields S and D provides the constitutive relations and the essential boundary conditions.

We decompose as follows the position vector x of a point, its mechanical displacement u, the electric displacement D, the body force b, the surface tractions t, and the outward unit normal n:

$$x = r + ze, \qquad u = v + we, \qquad n = \hat{n} + ne$$

$$D = \hat{D} + \delta e, \qquad b = \hat{b} + \beta e, \qquad t = \hat{t} + te \qquad (5)$$

where e is a unit vector along the positive x_3 axis. Thus, r is the projection of the position vector of a point on the x_1–x_2 plane, and v and w, respectively, equal its displacements in the x_1–x_2 plane and along the x_3 axis. Note that $v, w, \hat{n}, n, \hat{D}, \delta$, etc., are functions of r and z. The other field variables can now be written as

$$E(u) = \text{sym grad}\, v + [(v' + \text{grad}\, w)/2] \otimes e + e \otimes [(v' + \text{grad}\, w)/2]$$

$$+ w'e \otimes e = \hat{E} + \gamma \otimes e + e \otimes \gamma + \epsilon\, e \otimes e$$

$$W(\varphi) = -\text{grad}\, \varphi - \varphi'e = \hat{W} + \omega\, e$$

$$S = \hat{S} + s \otimes e + e \otimes s + \sigma\, e \otimes e \qquad (6)$$

where a prime indicates differentiation with respect to z, grad is the gradient operator in the x_1–x_2 plane, $a \otimes b$ denotes the tensor product between vectors a and b, $(a \otimes b)c = (b \cdot c)a$ for every vector c, γ is the transverse shear strain, ϵ is the transverse normal strain that describes the change in the thickness of the plate, ω is the electric field in the thickness direction, σ is the transverse normal stress, and s is the transverse shear stress. Furthermore, $\hat{S}$ is the in-plane (in the x_1–x_2 plane) stress tensor, $\hat{E}$ is the in-plane strain tensor, $\text{sym grad}\, v = [\text{grad}\, v + (\text{grad}\, v)^T]/2$, $\epsilon = w'$, $\omega = -\varphi'$, and $\hat{W} = -\text{grad}\, \varphi$. The constitutive relation (3) for the linear anisotropic PZT body can be written as

$$\begin{Bmatrix} \hat{E} \\ \gamma \\ \epsilon \\ \hat{W} \\ \omega \end{Bmatrix} = \begin{bmatrix} \mathbb{F}_{ES} & \mathbb{F}_{Es} & \mathbb{F}_{E\sigma} & \mathbb{M}_{ED} & \mathbb{M}_{E\delta} \\ * & \mathbb{F}_{\gamma s} & \mathbb{F}_{\gamma\sigma} & \mathbb{M}_{\gamma D} & \mathbb{M}_{\gamma\delta} \\ * & * & \mathbb{F}_{\epsilon\sigma} & \mathbb{M}_{\epsilon D} & \mathbb{M}_{\epsilon\delta} \\ * & * & * & \mathbb{N}_{WD} & \mathbb{N}_{W\delta} \\ * & * & * & * & \mathbb{N}_{\omega\delta} \end{bmatrix} \begin{Bmatrix} \hat{S} \\ s \\ \sigma \\ \hat{D} \\ \delta \end{Bmatrix} \qquad (7)$$

where an $*$ in row i and column j represents the transpose of the quantity in row j and column i of the matrix. Here $\hat{E}$ and $\hat{S}$ are three-dimensional vectors; γ, s, $\hat{W}$, and $\hat{D}$ are two-dimensional vectors; and ϵ, ω, σ, and δ are scalars. Furthermore, $\mathbb{F}_{ES}$, $\mathbb{F}_{Es}$, $\mathbb{F}_{E\sigma}$, $\mathbb{M}_{ED}$, $\mathbb{M}_{E\delta}$, $\mathbb{F}_{\gamma s}$, $\mathbb{F}_{\gamma\sigma}$, $\mathbb{M}_{\gamma D}$, $\mathbb{M}_{\gamma\delta}$, $\mathbb{F}_{\epsilon\sigma}$, $\mathbb{M}_{\epsilon D}$, $\mathbb{M}_{\epsilon\delta}$, $\mathbb{N}_{WD}$, $\mathbb{N}_{W\delta}$, $\mathbb{N}_{\omega\delta}$ are, respectively, 3×3, 3×2, 3×1, 3×2, 3×1, 2×2, 2×1, 2×2, 2×1, 1×1, 1×2, 1×1, 2×2, 2×1, and 1×1 matrices. These submatrices are derived from the matrices $\mathbb{F}$, $\mathbb{M}$, and $\mathbb{N}$ appearing in the constitutive relation (3). The functional $\mathfrak{H}$ now becomes

$$\mathfrak{H}(v, w, \hat{S}, s, \sigma, \varphi, \hat{D}, \delta) = \int_{\mathcal{C}} (\hat{b} \cdot v + \beta w) + \int_{\mathcal{C}} q\varphi$$

$$+ \int_{\partial_b \mathcal{C}} (\hat{t} \cdot v + tw) + \int_{\partial_\beta \mathcal{C}} \chi\varphi + \int_{\partial_a \mathcal{C}} [(\hat{S}\hat{n} + sn) \cdot (v - \bar{v})$$

$$+ (s \cdot \hat{n} + \sigma n)(w - \bar{w})] + \int_{\partial_a \mathcal{C}} [(\hat{D} \cdot \hat{n} + \delta n)(\varphi - \bar{\varphi})]$$

$$- \int_{\mathcal{C}} (\hat{S} \cdot \hat{E} + 2s \cdot \gamma + \sigma\epsilon) - \int_{\mathcal{C}} (\hat{D} \cdot \hat{W} + \delta\omega)$$

$$+ \frac{1}{2} \int_{\mathcal{C}} \hat{S} \cdot (\mathbb{F}_{ES}\hat{S} + \mathbb{F}_{Es}s + \mathbb{F}_{E\sigma}\sigma + \mathbb{M}_{ED}\hat{D} + \mathbb{M}_{E\delta}\delta)$$

$$+ \frac{1}{2} \int_{\mathcal{C}} s \cdot \left(\mathbb{F}_{Es}^\top \hat{S} + \mathbb{F}_{\gamma s}s + \mathbb{F}_{\gamma\sigma}\sigma + \mathbb{M}_{\gamma D}\hat{D} + \mathbb{M}_{\gamma\delta}\delta\right)$$

$$+ \frac{1}{2} \int_{\mathcal{C}} \sigma \left(\mathbb{F}_{E\sigma}^\top \hat{S} + \mathbb{F}_{\gamma\sigma}^\top s + \mathbb{F}_{\epsilon\sigma}\sigma + \mathbb{M}_{\epsilon D}\hat{D} + \mathbb{M}_{\epsilon\delta}\delta\right)$$

$$+ \frac{1}{2} \int_{\mathcal{C}} \hat{D} \cdot \left(\mathbb{N}_{WD}\hat{D} + \mathbb{N}_{W\delta}\delta + \mathbb{M}_{ED}^\top \hat{S} + \mathbb{M}_{\gamma D}^\top s + \mathbb{M}_{\epsilon D}^\top \sigma\right)$$

$$+ \frac{1}{2} \int_{\mathcal{C}} \delta\left(\mathbb{N}_{W\delta}^\top \hat{D} + \mathbb{N}_{\omega\delta}\delta + \mathbb{M}_{E\delta}^\top \hat{S} + \mathbb{M}_{\gamma\delta}^\top s + \mathbb{M}_{\epsilon\delta}^\top \sigma\right) \qquad (8)$$

III. Derivation of a Higher-Order Plate Theory

Let P^K be the space of the Kth-order polynomials defined on the interval $[-1, 1]$. We choose Legendre polynomials, $L_0(z)$, $L_1(z)$, $\ldots$, $L_K(z)$, normalized according to relation (9), as the basis functions in P^K:

$$\langle L_i, L_j \rangle := \int_{-1}^{1} L_i(z) L_j(z) dz = \delta_{ij}, \qquad i, j = 0, 1, 2, \ldots, K \tag{9}$$

where δ_{ij} is the Kronecker delta. We note that

$$L_0(z) = \frac{1}{\sqrt{2}}, \qquad L_1(z) = \sqrt{\tfrac{3}{2}}z, \qquad L_2(z) = \sqrt{\tfrac{5}{2}}(3z^2 - 1)/2$$

$$L_3(z) = \sqrt{\tfrac{7}{2}}(-3z/2 + 5z^3/2), \ldots \tag{10}$$

The displacement fields v and w and the electric potential φ are approximated by the following series:

$$v(\mathbf{r}, z) = L_i(z)v_i(\mathbf{r}) \tag{11a}$$

$$w(\mathbf{r}, z) = L_i(z)w_i(\mathbf{r}) \tag{11b}$$

$$\varphi(\mathbf{r}, z) = L_i(z)\varphi_i(\mathbf{r}) \tag{11c}$$

Here and hereafter, a repeated index implies summation over the range of the index. Indices i and j range over $0, 1, 2, \ldots, K$. Mindlin and Medick[10] derived a plate theory by using expansions (11a) and (11b) with $K = \infty$ for the mechanical displacements and employed the principle of virtual work. For the mechanical problem, they substituted expressions (13) for strains in the constitutive relation (3), written as $S = \mathbb{F}^{-1}E$, and obtained expressions for stresses $S_0, S_1, S_2, \ldots$, for plate theories of different order. They vividly show the displacements and stresses of order 0, 1, and 2. Lee and Yu[16] expanded the three components of the mechanical displacement, the electric potential, and the material parameters as power

series in z and used a variational principle to derive the equations of motion for a functionally graded PZT plate. Two-dimensional constitutive relations of order n for a homogeneous plate involve displacements and the electric potential of all orders up to ∞. They deduce a first-order theory by retaining terms v_0, v_1, w_0, w_1, w_2, ϕ_0, and ϕ_1 in Eqs. (11), stresses and strains up to order one, electric displacements and electric fields up to order three, and introduce correction factors to match the frequencies of the simple thickness vibrations computed from the first-order theory with those from the three-dimensional equations. Their approach is similar to that of Mindlin and Medick.[10] Even though the basis functions $(1, z, z^2, \ldots)$ and $[L_0(z), L_1(z), L_2(z), \ldots]$ are equivalent, the latter set results in simpler equations because the Legendre polynomials are mutually orthogonal. Lee et al.[17] used trigonometric basis function $[\cos(K\pi/2)(1 - z)]$ to expand the three components of the mechanical displacement and the electric potential. Because of the orthogonal properties of the trigonometric functions, the algebraic work is simplified. Whereas in the present Kth-order plate theory the kinematic variables are expressed as a polynomial in z of degree K, in the Lee et al.[17] work even a first-order plate theory involves terms in z^K with $K > 1$ because of the trigonometric basis functions used. The present work differs from that of Mindlin and Medick[10] and Lee and Yu[16] in the derivation of the constitutive relations. Because of the finite series considered in Eq. (11), there is no truncation to be done. In the first- and the third-order shear deformation theories, the transverse component w of the mechanical displacement is usually assumed to be independent of z and the two in-plane components, respectively, polynomials of degree one and three in z. Three-dimensional analytical solutions[20] show that for thick laminates the plate thickness changes, and the variation of the transverse shear stress through the thickness of the plate cannot be described by a polynomial of degree two in z.

Recalling that $L_i'(z)$ is a polynomial of degree $(i - 1)$, we write it as

$$L_i'(z) = D_{ij} L_j(z) \tag{12}$$

where D_{ij} are constants. Note that the last column of the $(K + 1) \times (K + 1)$ matrix D_{ij} is identically zero. Substitution for v, w, and φ from Eqs. (11) into Eqs. (6) yields

$$\hat{E} = L_i(z) \, \text{sym grad} \, v_i =: L_i(z)\hat{E}_i \tag{13a}$$

$$\gamma = L_i(z)[(D_{ji}v_j + \text{grad}\, w_i)/2] =: L_i(z)\gamma_i \tag{13b}$$

$$\epsilon = L_i(z)D_{ji}w_j =: L_i(z)\epsilon_i \tag{13c}$$

$$\hat{W} = -L_i(z) \, \text{grad} \, \varphi_i =: L_i(z)\hat{W}_i \tag{13d}$$

$$\omega = -L_i(z)D_{ji}\varphi_j =: L_i(z)\omega_i \tag{13e}$$

We now substitute for $\hat{E}$, γ, ϵ, $\hat{W}$, and ω from Eqs. (13) into the right-hand side of Eq. (8) and integrate with respect to z to arrive at the following expression for the functional $\mathfrak{H}$:

$$\mathfrak{H} = \int_{\mathcal{S}} (\mathbf{B}_i \cdot v_i + \Xi_i w_i + Q_i \varphi_i) + \int_{\partial_b \mathcal{S}} (\mathbf{F}_i \cdot v_i + \Phi_i w_i)$$

$$+ \int_{\partial_\beta \mathcal{S}} (X_i \varphi_i) + \int_{\mathcal{S}} [(\text{div}\, \mathbf{N}_i - D_{ji}\mathbf{T}_j) \cdot v_i + (\text{div}\, \mathbf{T}_i - D_{ji}\Sigma_j)w_i$$

$$+ (\text{div}\, \mathbf{\Delta}_i - D_{ji}d_j)\varphi_i] + \int_{\partial_b \mathcal{S}} [(\mathbf{N}_i \hat{n}) \cdot v_i + (\mathbf{T}_i \cdot \hat{n})w_i]$$

$$- \int_{\partial_\beta \mathcal{S}} [(\mathbf{\Delta}_i \cdot \hat{n})\varphi_i] + \mathfrak{R}(\hat{S}, s, \sigma, \hat{D}, \delta) \tag{14}$$

Here,

$$\mathbf{B}_i = \langle L_i, \hat{b} \rangle + L_i(1)\hat{t}^+ + L_i(-1)\hat{t}^- \tag{15a}$$

$$\Xi_i = \langle L_i, \beta \rangle + L_i(1)t^+ + L_i(-1)t^- \tag{15b}$$

$$Q_i = \langle L_i, q \rangle + L_i(1)\chi^+ + L_i(-1)\chi^- \tag{15c}$$

$$F_i = \langle L_i, \hat{t} \rangle \tag{15d}$$

$$\Phi_i = \langle L_i, t \rangle \tag{15e}$$

$$X_i = \langle L_i, \chi \rangle \tag{15f}$$

$$N_i = \langle L_i, \hat{S} \rangle \tag{15g}$$

$$T_i = \langle L_i, s \rangle \tag{15h}$$

$$\Sigma_i = \langle L_i, \sigma \rangle \tag{15i}$$

$$\Delta_i = \langle L_i, \hat{D} \rangle \tag{15j}$$

$$d_i = \langle L_i, \delta \rangle \tag{15k}$$

and $\mathfrak{R}(\hat{S}, s, \sigma, \hat{D}, \delta)$ is the part of $\mathfrak{H}$ that does not depend on the mechanical displacements and the electric potential. Superscripts $+$ and $-$ on a quantity signify its values on surfaces $\mathcal{S}^+$ and $\mathcal{S}^-$, respectively. Furthermore, N_i is a 2×2 symmetric matrix; N_0 gives the in-plane (within the plane $\mathcal{S}$) forces (sometimes also called the membranal stress tensor); N_1 is the matrix of bending moments (also called the moment tensor); the matrix N_i ($i = 2, 3, \ldots, K$) comprises a linear combination of matrices of bending moments of order zero through i; T_0 is the resultant shear force or the shear stress vector; T_1 is the moment of the internal double forces (i.e., forces acting along the normal e to the midsurface of the plate); T_i ($i = 2, 3, \ldots, K$) equals the linear combination of the moments up to ith order of the internal double forces; Σ_0 is the resultant transverse normal stress; and Σ_i ($i = 1, 2, 3, \ldots, K$) is the linear combination of the moments up to the ith order of the transverse normal stress. Δ_0 is the resultant in-plane electric displacement, Δ_1 represents the moment of order one of the in-plane electric displacement, and Δ_i equals the linear combination of the moments up to order i of the in-plane electric displacement. Similar interpretations hold for the other quantities. Note that the surface tractions and the normal component of the electric displacement prescribed on the top and the bottom surfaces of the plate appear in the definitions of B_i, Ξ_i, and Q_i [cf. Eqs. (15a–15c)]. Because of the relation $L_i(-1) = (-1)^i L_i(1)$ in which the index i is not summed, the contributions of the normal surface tractions on the upper and the lower surfaces can be written as

$$L_i(1)t^+ + L_i(-1)t^- = \begin{cases} L_i(1)(t^+ + t^-), & i = 0, 2, \ldots \\ L_i(1)(t^+ - t^-), & i = 1, 3, \ldots \end{cases} \tag{16}$$

and analogous expressions hold for $\hat{t}$ and χ.

The variation of $\mathfrak{H}$ with respect to v_i, w_i, and φ_i gives

$$\operatorname{div} N_i - D_{ji} T_j + B_i = 0 \tag{17a}$$

$$\operatorname{div} T_i - D_{ji} \Sigma_j + \Xi_i = 0 \tag{17b}$$

$$\operatorname{div} \Delta_i - D_{ji} d_j + Q_i = 0 \tag{17c}$$

on $\mathcal{S}$,

$$N_i \hat{n} = F_i, \qquad T_i \cdot \hat{n} = \Phi_i, \tag{18a}$$

on $\partial_b \mathcal{S}$,

$$\Delta_i \cdot \hat{n} = X_i, \qquad i = 0, 1, 2, \ldots, K \tag{18b}$$

on $\partial_\beta \mathcal{S}$. These are the balance equations and the natural boundary conditions for the plate theory. Equations (17a) and (17b) are clearly coupled because of the presence of the moments T_i of the internal double force in both equations. Because the matrix D_{ij} is nondiagonal, $T_0, T_1, \ldots, T_K, \Sigma_0, \Sigma_1, \ldots, \Sigma_K, d_0, d_1, \ldots, d_K$ will appear in Eqs. (17a–17c), respectively. Thus, to solve the problem for the Kth-order theory, the $3(K + 1)$ equations (17) need to be solved simultaneously. The electromechanical coupling effects are exhibited through the dependence of the kinetic fields N_i, T_i, Σ_i, Δ_i, and d_i on the kinematic variables $\hat{E}_i$, γ_i, ϵ_i, $\hat{W}_i$, and ω_i in the constitutive relations derived hereafter.

For $i = 0, 1, 2, \ldots, K$, we have $3(K + 1)$ equilibrium equations (17) defined on the midsurface $\mathcal{S}$ of the plate and the corresponding natural boundary conditions (18) on $\partial \mathcal{S}$. From the prescribed fields of the body force b, surface tractions t, and the charge density χ, we can compute the fields B_i, Ξ_i, Q_i, F_i, Φ_i, and X_i defined on $\mathcal{S}$. To complete the plate theory, we need to derive constitutive relations for N_i, T_i, Δ_i, Σ_i, and d_i and the essential boundary conditions on $\partial \mathcal{S}$.

For the kinetic fields S and D, we choose an expansion that satisfies Eqs. (15g–15k) and the boundary conditions

$$s(r, \pm 1) = \pm \hat{t}^\pm, \qquad \sigma(r, \pm 1) = \pm t^\pm, \qquad \delta(r, \pm 1) = \pm \chi^\pm \tag{19}$$

on the upper and the lower surfaces of the plate; an entry in Eq. (19) should be read as $s(r, +1) = +\hat{t}^+$. Among various ways of achieving this goal, we consider two alternatives.

As the first choice, we set

$$\hat{S}(r, z) = L_i(z)N_i(r) \tag{20a}$$

$$s(r, z) = \tilde{L}_i(z)T_i(r) + \tilde{L}_+(z)\hat{t}^+(r) + \tilde{L}_-(z)\hat{t}^-(r) \tag{20b}$$

$$\sigma(r, z) = \tilde{L}_i(z)\Sigma_i(r) + \tilde{L}_+(z)t^+(r) + \tilde{L}_-(z)t^-(r) \tag{20c}$$

$$\hat{D}(r, z) = L_i(z)\Delta_i(r) \tag{20d}$$

$$\delta(r, z) = \tilde{L}_i(z)d_i(r) + \tilde{L}_+(z)\chi^+(r) + \tilde{L}_-(z)\chi^-(r) \tag{20e}$$

where

$$\langle \tilde{L}_i, L_j \rangle = \delta_{ij} \tag{21a}$$

$$\tilde{L}_i(\pm 1) = 0, \qquad i, j = 0, 1, 2, \ldots, K \tag{21b}$$

$$\langle \tilde{L}_\pm, L_i \rangle = 0 \tag{21c}$$

$$\tilde{L}_+(\pm 1) = \begin{cases} 1 \\ 0 \end{cases} \tag{21d}$$

$$\tilde{L}_-(\pm 1) = \begin{cases} 0 \\ -1 \end{cases} \tag{21e}$$

Note that $\tilde{L}_+(z)$, $\tilde{L}_-(z)$, and $\tilde{L}_i(z)$, $i = 0, 1, 2, \ldots, K$, defined on $[-1, 1]$, form basis functions for the space of polynomials of degree $K + 2$, that is, they are linearly independent.

Substitution from Eqs. (20) into Eq. (8) and the variation of $\mathfrak{H}$ with respect to N_i, T_i, Σ_i, Δ_i, and d_i give the following constitutive relations and the essential boundary conditions:

$$\hat{E}_i = \mathbb{F}_{ES} N_i + \mathbb{F}_{Es} T_i + \mathbb{F}_{E\sigma} \Sigma_i + \mathbb{M}_{ED} \Delta_i + \mathbb{M}_{E\delta} d_i$$

$$\gamma_i = \mathbb{F}_{Es}^\top N_i + \mathbb{F}_{\gamma s} P_{ij} T_j + \mathbb{F}_{\gamma \sigma} P_{ij} \Sigma_j + \mathbb{M}_{\gamma D} \Delta_i + \mathbb{M}_{\gamma \delta} P_{ij} d_j$$
$$\quad + P_{i\pm} \left(\mathbb{F}_{\gamma s} \hat{t}^\pm + \mathbb{F}_{\gamma \sigma} t^\pm + \mathbb{M}_{\gamma \delta} \chi^\pm \right)$$

$$\epsilon_i = \mathbb{F}_{E\sigma}^\top N_i + \mathbb{F}_{\gamma \sigma}^\top P_{ij} T_j + \mathbb{F}_{\epsilon \sigma} P_{ij} \Sigma_j + \mathbb{M}_{\epsilon D} \Delta_i + \mathbb{M}_{\epsilon \delta} P_{ij} d_j$$
$$\quad + P_{i\pm} \left(\mathbb{F}_{\gamma \sigma}^\top \hat{t}^\pm + \mathbb{F}_{\epsilon \sigma} t^\pm + \mathbb{M}_{\epsilon \delta} \chi^\pm \right)$$

$$\hat{W}_i = \mathbb{N}_{WD} \Delta_i + \mathbb{N}_{W\delta} d_i + \mathbb{M}_{ED}^\top N_i + \mathbb{M}_{\gamma D}^\top T_i + \mathbb{M}_{\epsilon D}^\top \Sigma_i$$

$$\omega_i = \mathbb{N}_{W\delta}^\top \Delta_i + \mathbb{N}_{\omega \delta} P_{ij} d_j + \mathbb{M}_{E\delta}^\top N_i + \mathbb{M}_{\gamma \delta}^\top P_{ij} T_j + \mathbb{M}_{\epsilon \delta}^\top P_{ij} \Sigma_j$$
$$\quad + P_{i\pm} \left(\mathbb{N}_{\omega \delta} \chi^\pm + \mathbb{M}_{\gamma \delta}^\top \hat{t}^\pm + \mathbb{M}_{\epsilon \delta}^\top t^\pm \right) \tag{22}$$

$$v_i = \tilde{\tilde{v}}_i, \qquad w_i = \tilde{\tilde{w}}_i \tag{23a}$$

on $\partial_a \mathcal{S}$

$$\varphi_i = \tilde{\tilde{\varphi}}_i \tag{23b}$$

on $\partial_\alpha \mathcal{S}$ where

$$P_{ij} := \langle \tilde{L}_i, \tilde{L}_j \rangle \tag{24a}$$

$$P_{i\pm} := \langle \tilde{L}_i, \tilde{L}_\pm \rangle, \qquad i, j = 0, 1, 2, \ldots, K \tag{24b}$$

$$\tilde{\bar{v}}_i = \langle L_i, \bar{v} \rangle \tag{24c}$$

$$\tilde{\bar{w}}_i = \langle \tilde{L}_i, \bar{w} \rangle \tag{24d}$$

$$\tilde{\bar{\varphi}}_i = \langle \tilde{L}_i, \bar{\varphi} \rangle \tag{24e}$$

It is clear from Eqs. (22) that components of the ith-order in-plane strain tensor and components of the ith-order in-plane electric displacement depend on components of the ith-order kinetic variables N, T, Σ, Δ, and d. However, components of the ith-order transverse shear strain γ, the ith-order transverse normal strain ϵ, and the ith-order transverse electric displacement ω depend in general on the components of N, T, Σ, Δ, and d up to the Kth order. This is because P_{ij} is a nondiagonal matrix.

Balance laws (17), constitutive relations (22), boundary conditions (18) and (23), and strain-displacement relations (13) form a complete set of equations for a plate problem. Because of the property $P_{i-} = (-1)^{i+1} P_{i+}$, the contributions to the constitutive relations of the normal surface tractions on the upper and the lower surfaces can be written as

$$P_{i\pm} t^\pm := P_{i+} t^+ + P_{i-} t^- = \begin{cases} P_{i+}(t^+ - t^-), & i = 0, 2, \ldots, \\ P_{i+}(t^+ + t^-), & i = 1, 3, \ldots, \end{cases} \tag{25}$$

and analogous expressions hold for $\hat{t}$ and χ.

For a PZT plate, the principle of virtual work can be stated as

$$\int_{\mathcal{S}} (\boldsymbol{B}_i \cdot \delta \boldsymbol{v}_i + \Xi_i \delta w_i + Q_i \delta \varphi_i) + \int_{\partial_b \mathcal{S}} (\boldsymbol{F}_i \cdot \delta \boldsymbol{v}_i + \Phi_i \delta w_i)$$

$$+ \int_{\partial_\beta \mathcal{S}} (X_i \delta \varphi_i) = \int_{\mathcal{S}} [\boldsymbol{N}_i \cdot \delta \hat{\boldsymbol{E}}_i + \boldsymbol{T}_i \cdot \delta \boldsymbol{\gamma}_i$$

$$+ \Sigma_i \delta \epsilon_i + \boldsymbol{\Delta}_i \cdot \delta \hat{\boldsymbol{W}}_i + d_i \delta \omega_i] \tag{26}$$

must hold for all virtual fields $\{\delta \hat{\boldsymbol{E}}_i, \delta \boldsymbol{\gamma}_i, \delta \epsilon_i, \delta \hat{\boldsymbol{W}}_i, \delta \omega_i\}$ with fields $\{\delta \boldsymbol{v}_i, \delta w_i, \delta \varphi_i\}$ vanishing on those parts of the boundary where essential boundary conditions (23) are specified.

The polynomial functions $\tilde{L}_\pm(z)$ of degree $K+2$ in z exhibit oscillatory behavior for large values of K. Accordingly, we modify the expressions (20b), (20c), and (20e) for $s(\boldsymbol{r}, z)$, $\sigma(\boldsymbol{r}, z)$ and $\delta(\boldsymbol{r}, z)$ to those given hereafter, and this is our second choice of constitutive relations:

$$s(\boldsymbol{r}, z) = \tilde{L}_i(z) \tilde{\boldsymbol{T}}_i(\boldsymbol{r}) + \alpha_0 L_0(z) \hat{\boldsymbol{t}}_0(\boldsymbol{r}) + \alpha_1 L_1(z) \hat{\boldsymbol{t}}_1(\boldsymbol{r})$$

$$\sigma(\boldsymbol{r}, z) = \tilde{L}_i(z) \tilde{\Sigma}_i(\boldsymbol{r}) + \alpha_0 L_0(z) t_0(\boldsymbol{r}) + \alpha_1 L_1(z) t_1(\boldsymbol{r})$$

$$\delta(\boldsymbol{r}, z) = \tilde{L}_i(z) \tilde{d}_i(\boldsymbol{r}) + \alpha_0 L_0(z) \chi_0(\boldsymbol{r}) + \alpha_1 L_1(z) \chi_1(\boldsymbol{r}) \tag{27}$$

where

$$\hat{\boldsymbol{t}}_0(\boldsymbol{r}) := (\hat{\boldsymbol{t}}^+ - \hat{\boldsymbol{t}}^-)/2, \qquad \hat{\boldsymbol{t}}_1(\boldsymbol{r}) := (\hat{\boldsymbol{t}}^+ + \hat{\boldsymbol{t}}^-)/2$$

$$t_0(\boldsymbol{r}) := (t^+ - t^-)/2, \qquad t_1(\boldsymbol{r}) := (t^+ + t^-)/2$$

$$\chi_0(\boldsymbol{r}) := (\chi^+ - \chi^-)/2, \qquad \chi_1(\boldsymbol{r}) := (\chi^+ + \chi^-)/2 \tag{28}$$

For Eqs. (27) to satisfy the natural boundary conditions (19), we have

$$\alpha_0 = 1/L_0(1), \qquad \alpha_1 = 1/L_1(1) \tag{29}$$

Note that $\tilde{L}_i(z)$, $i = 0, 1, 2, \ldots, K$, $L_0(z)$, and $L_1(z)$ form basis functions in the space of polynomials of degree $K+2$.

Equations (15h), (15i), (15k), and (27) imply that

$$\boldsymbol{T}_0 = \tilde{\boldsymbol{T}}_0 + \alpha_0 \hat{t}_0, \qquad \boldsymbol{T}_1 = \tilde{\boldsymbol{T}}_1 + \alpha_1 \hat{t}_1, \qquad \boldsymbol{T}_i = \tilde{\boldsymbol{T}}_i$$

$$\Sigma_0 = \tilde{\Sigma}_0 + \alpha_0 t_0, \qquad \Sigma_1 = \tilde{\Sigma}_1 + \alpha_1 t_1, \qquad \Sigma_i = \tilde{\Sigma}_i$$

$$d_0 = \tilde{d}_0 + \alpha_0 \chi_0, \qquad d_1 = \tilde{d}_1 + \alpha_1 \chi_1, \qquad d_i = \tilde{d}_i$$

$$i = 2, 3, \ldots, K \tag{30}$$

The variation of $\mathfrak{H}$ with respect to N_i, $\tilde{\boldsymbol{T}}_i$, $\tilde{\Sigma}_i$, $\boldsymbol{\Delta}_i$, and $\tilde{d}_i$ gives boundary conditions (23) and the following constitutive relations:

$$\begin{Bmatrix} \hat{\boldsymbol{E}}_i \\ \gamma_i \\ \epsilon_i \\ \hat{\boldsymbol{W}}_i \\ \omega_i \end{Bmatrix} = \begin{pmatrix} \mathbb{F}_{ES}\delta_{ij} & \mathbb{F}_{Es}\delta_{ij} & \mathbb{F}_{E\sigma}\delta_{ij} & \mathbb{M}_{ED}\delta_{ij} & \mathbb{M}_{E\delta}\delta_{ij} \\ * & \mathbb{F}_{\gamma s}P_{ij} & \mathbb{F}_{\gamma\sigma}P_{ij} & \mathbb{M}_{\gamma D}\delta_{ij} & \mathbb{M}_{\gamma\delta}\delta_{ij} \\ * & * & \mathbb{F}_{\epsilon\sigma}P_{ij} & \mathbb{M}_{\epsilon D}\delta_{ij} & \mathbb{M}_{\epsilon\delta}P_{ij} \\ * & * & * & \mathbb{N}_{WD}\delta_{ij} & \mathbb{N}_{W\delta}\delta_{ij} \\ * & * & * & * & \mathbb{N}_{\omega\delta}P_{ij} \end{pmatrix} \begin{Bmatrix} N_j \\ T_j \\ \Sigma_j \\ \Delta_j \\ d_j \end{Bmatrix}$$

$$+ \begin{Bmatrix} \mathbf{0} \\ (\delta_{ij} - P_{ij})(\alpha_j \mathbb{F}_{\gamma s}\hat{t}_i + \alpha_j \mathbb{F}_{\gamma\sigma}t_i + \alpha_j \mathbb{M}_{\gamma\delta}\chi_i) \\ (\delta_{ij} - P_{ij})(\alpha_j \mathbb{F}_{\gamma\sigma}^\top \hat{t}_i + \alpha_j \mathbb{F}_{\epsilon\sigma}t_i + \alpha_j \mathbb{M}_{\epsilon\delta}\chi_i) \\ \mathbf{0} \\ (\delta_{ij} - P_{ij})(\alpha_j \mathbb{N}_{\omega\delta}\chi_i + \alpha_j \mathbb{M}_{\gamma\delta}^\top \hat{t}_i + \alpha_j \mathbb{M}_{\epsilon\delta}^\top t_i) \end{Bmatrix} \tag{31}$$

where $\alpha_i = 0$, for $i = 2, \ldots, K$. Note that in the second term on the right-hand side of Eq. (31) the index i is not summed but that the summation convention applies to the repeated index j. By using relations (30), Eqs. (27) can be written as

$$s(\boldsymbol{r}, z) = \tilde{L}_i(z) \boldsymbol{T}_i(\boldsymbol{r}) + \alpha_0 [L_0(z) - \tilde{L}_0(z)] \hat{t}_0(\boldsymbol{r})$$

$$+ \alpha_1 [L_1(z) - \tilde{L}_1(z)] \hat{t}_1(\boldsymbol{r})$$

$$\sigma(\boldsymbol{r}, z) = \tilde{L}_i(z) \Sigma_i(\boldsymbol{r}) + \alpha_0 [L_0(z) - \tilde{L}_0(z)] t_0(\boldsymbol{r})$$

$$+ \alpha_1 [L_1(z) - \tilde{L}_1(z)] t_1(\boldsymbol{r})$$

$$\delta(\boldsymbol{r}, z) = \tilde{L}_i(z) d_i(\boldsymbol{r}) + \alpha_0 [L_0(z) - \tilde{L}_0(z)] \chi_0(\boldsymbol{r})$$

$$+ \alpha_1 [L_1(z) - \tilde{L}_1(z)] \chi_1(\boldsymbol{r}) \tag{32}$$

Balance laws (17), constitutive relations (22) or (31), boundary conditions (18) and (23), and strain-displacement relations (13) form a complete set of equations for a plate problem. For a transversely isotropic or an orthotropic piezoceramic plate, Eqs. (22) or (31) can be readily inverted to solve for N_i, $\boldsymbol{T}_i$, Σ_i, $\boldsymbol{\Delta}_i$, and d_i in terms of $\hat{\boldsymbol{E}}_i$, $\boldsymbol{\delta}_i$, ϵ_i, $\hat{\boldsymbol{W}}_i$, and ω_i; however, these inversions can always be performed numerically. These relations, when substituted into the balance laws (17), will give $4(K+1)$ coupled second-order partial differential equations for the $4(K+1)$ unknowns v_i, ω_i, and ϕ_i, $i = 0, 1, 2, \ldots, K$. Hence, Lagrange basis functions can be used to solve the resulting boundary-value problems by the finite element method. For $K = 1$, the present plate theory differs from the first-order shear deformation theory (FSDT) in the following two respects. Whereas we account for the transverse normal strains, the FSDT does not. Also, in the FSDT the transverse shear stresses are taken to be polynomials of first degree in z, and the transverse normal stresses are omitted and subsequently computed by integrating the three-dimensional elasticity equations. Here, these stress components are expressed as polynomials of degree three in z and the stress components are computed from Eqs. (20) or (27).

With the appropriate definitions of the gradient and the divergence operators in cylindrical and elliptic coordinates, Eqs. (17) and (22) or (31), (18), (23), and (13) can be written for circular and elliptic plates. Governing equations for the transient electromechanical deformations of a plate are obtained when the body force $\boldsymbol{b}$ is replaced by $\bar{\boldsymbol{b}} - \rho \ddot{\boldsymbol{u}}$, where $\bar{\boldsymbol{b}}$ is the density of the external body force, ρ is the mass density, and a superimposed dot indicates the time derivative; see Batra et al.[21]

IV. Results for Example Problems

In the four example problems studied hereafter, a plane state of stress is assumed to prevail in the x_1–x_3 plane. Thus, the dimension of the plate in the x_2 direction is much smaller than its dimensions in the x_1 and x_3 directions. It is usual to call such a plate a beam. The 2×2 in-plane stress tensor $\hat{S}$ has only one nonvanishing component $\hat{S}_{11}$, and the nonzero component of the transverse shear stress s is s_1. The other nonzero component of the stress tensor is the transverse normal stress σ.

A. Mechanical Problem
1. Thick Cantilever Beam Loaded by Uniformly Distributed Normal Tractions on Its Top and Bottom Surfaces

We analyze mechanical deformations of a homogeneous, orthotropic graphite-epoxy cantilever thick beam of length equal to twice its thickness. There is no body force, and the beam is loaded by a uniformly distributed normal traction, $q_0/2$, on its upper and lower surfaces $\mathcal{S}^+$ and $\mathcal{S}^-$, respectively. The edge $x_1 = 0$ of the beam is clamped, and the other edge $x_1 = L$ is traction free. This example problem provides a good test of the plate theory for thick laminates. Vel and Batra[22] have found an analytical solution of the problem based on the assumption of a generalized plane strain state of deformation. For an elastic problem, the compliance matrices for the two states of deformation are related to each other.

The boundary conditions for the problem are

$$t^+ = q_0/2, \qquad \hat{t} = 0 \text{ on } \mathcal{S}^+, \qquad t^- = q_0/2, \qquad \hat{t} = 0 \text{ on } \mathcal{S}^-$$

$$\bar{v} = 0, \qquad \bar{w} = 0 \text{ on the edge } x_1 = 0$$

$$\hat{t} = 0, \qquad t = 0, \qquad \text{on the edge } x_1 = L \qquad (33)$$

Thus, the uniformly distributed load on the upper and the lower surfaces of the beam points in the positive x_3 direction. We give hereafter the balance laws (17), constitutive relations (31), strain-displacement relations (13), and boundary conditions (18) and (23) for $K = 3$ even though results have also been computed for K varying up to 7. Expressions for L_0, L_1, L_2, and L_3 are given in Eqs. (8). The solution of Eqs. (21a) and (21b) is

$$\tilde{L}_0(z) = \tfrac{\sqrt{2}}{16}(5 + 30z^2 - 35z^4)$$

$$\tilde{L}_1(z) = \tfrac{1}{16}\sqrt{\tfrac{2}{3}}(-21z + 210z^3 - 189z^5)$$

$$\tilde{L}_2(z) = \tfrac{1}{16}\sqrt{\tfrac{2}{5}}(-35 + 210z^2 - 175z^4)$$

$$\tilde{L}_3(z) = \tfrac{1}{16}\sqrt{\tfrac{2}{7}}(-189z + 630z^3 - 441z^5)$$

The matrices D_{ij} and P_{ij} defined, respectively, in Eqs. (12) and (24a) are

$$D = \begin{pmatrix} 0 & 0 & 0 & 0 \\ \sqrt{3} & 0 & 0 & 0 \\ 0 & \sqrt{15} & 0 & 0 \\ \sqrt{7} & 0 & \sqrt{35} & 0 \end{pmatrix}, \qquad P = \begin{pmatrix} \frac{10}{9} & 0 & \frac{\sqrt{5}}{9} & 0 \\ 0 & \frac{14}{11} & 0 & \frac{\sqrt{21}}{11} \\ \frac{\sqrt{5}}{9} & 0 & \frac{14}{9} & 0 \\ 0 & \frac{\sqrt{21}}{11} & 0 & \frac{18}{11} \end{pmatrix}$$

$$(34)$$

Expressions for L_4, L_5, L_6, L_7, $\tilde{L}_i$, D_{ij}, and P_{ij} for $K \le 7$ are given in the Appendix.

Because of the assumption of the plane state of stress in the x_1–x_3 plane, tensors N_i, T_i, and v_i, $i = 0, 1, 2, \ldots, K$, reduce to scalars, and their values vary only in the x_1 direction. Henceforth, we denote their derivatives with respect to x_1 by a prime, that is, $N_i' = \mathrm{d}N_i/\mathrm{d}x_1$. Our goal is to find v_i and w_i, $i = 0, 1, 2, 3$, as a function of x_1. The balance laws (17) take the form

$$N_0' = 0, \qquad T_0' + q_0/\sqrt{2} = 0, \qquad N_1' - \sqrt{3}T_0 = 0$$

$$T_1' - \sqrt{3}\Sigma_0 = 0, \qquad N_2' - \sqrt{15}T_1 = 0$$

$$T_2' - \sqrt{15}\Sigma_1 + \sqrt{\tfrac{5}{2}}q_0 = 0, \qquad N_3' - \sqrt{7}T_0 - \sqrt{35}T_2 = 0$$

$$T_3' - \sqrt{7}\Sigma_0 - \sqrt{35}\Sigma_2 = 0, \qquad 0 < x_1 < L \qquad (35)$$

Boundary conditions (23) and (18) reduce to

$$v_0 = v_1 = v_2 = v_3 = w_0 = w_1 = w_2 = w_3 = 0 \quad \text{at} \quad x_1 = 0$$

$$N_0 = N_1 = N_2 = N_3 = T_0 = T_1 = T_2 = T_3 = 0 \quad \text{at} \quad x_1 = L$$

$$(36)$$

For mechanical deformations in the x_1–x_3 plane, only the 11th component of $\hat{E}_i$ and the first component of γ_i need to be computed; these are denoted as scalars hereafter, and the suffixes 11 and 1 are dropped. The constitutive relation (31) simplifies to

$$\begin{Bmatrix} \hat{E}_0 \\ \gamma_0 \\ \epsilon_0 \end{Bmatrix} = \begin{bmatrix} \mathbb{F}_{ES} & \mathbb{F}_{Es} & \mathbb{F}_{E\sigma} \\ \mathbb{F}_{Es} & \frac{10}{9}\mathbb{F}_{\gamma s} & \frac{10}{9}\mathbb{F}_{\gamma \sigma} \\ \mathbb{F}_{E\sigma} & \frac{10}{9}\mathbb{F}_{\gamma \sigma} & \frac{10}{9}\mathbb{F}_{\epsilon \sigma} \end{bmatrix} \begin{Bmatrix} N_0 \\ T_0 \\ \Sigma_0 \end{Bmatrix}$$

$$+ \frac{\sqrt{5}}{9}\begin{bmatrix} 0 & 0 & 0 \\ 0 & \mathbb{F}_{\gamma s} & \mathbb{F}_{\gamma \sigma} \\ 0 & \mathbb{F}_{\gamma \sigma} & \mathbb{F}_{\epsilon \sigma} \end{bmatrix} \begin{Bmatrix} N_2 \\ T_2 \\ \Sigma_2 \end{Bmatrix}$$

$$\begin{Bmatrix} \hat{E}_1 \\ \gamma_1 \\ \epsilon_1 \end{Bmatrix} = \begin{bmatrix} \mathbb{F}_{ES} & \mathbb{F}_{Es} & \mathbb{F}_{E\sigma} \\ \mathbb{F}_{Es} & \frac{14}{11}\mathbb{F}_{\gamma s} & \frac{14}{11}\mathbb{F}_{\gamma \sigma} \\ \mathbb{F}_{E\sigma} & \frac{14}{11}\mathbb{F}_{\gamma \sigma} & \frac{14}{11}\mathbb{F}_{\epsilon \sigma} \end{bmatrix} \begin{Bmatrix} N_1 \\ T_1 \\ \Sigma_1 \end{Bmatrix}$$

$$+ \frac{\sqrt{21}}{11}\begin{bmatrix} 0 & 0 & 0 \\ 0 & \mathbb{F}_{\gamma s} & \mathbb{F}_{\gamma \sigma} \\ 0 & \mathbb{F}_{\gamma \sigma} & \mathbb{F}_{\epsilon \sigma} \end{bmatrix} \begin{Bmatrix} N_3 \\ T_3 \\ \Sigma_3 \end{Bmatrix} - \sqrt{\tfrac{3}{2}}\frac{q_0}{11}\begin{Bmatrix} 0 \\ \mathbb{F}_{\gamma s} \\ \mathbb{F}_{\epsilon \sigma} \end{Bmatrix}$$

$$\begin{Bmatrix} \hat{E}_2 \\ \gamma_2 \\ \epsilon_2 \end{Bmatrix} = \frac{\sqrt{5}}{9}\begin{bmatrix} 0 & 0 & 0 \\ 0 & \mathbb{F}_{\gamma s} & \mathbb{F}_{\gamma \sigma} \\ 0 & \mathbb{F}_{\gamma \sigma} & \mathbb{F}_{\epsilon \sigma} \end{bmatrix} \begin{Bmatrix} N_0 \\ T_0 \\ \Sigma_0 \end{Bmatrix}$$

$$+ \begin{bmatrix} \mathbb{F}_{ES} & \mathbb{F}_{Es} & \mathbb{F}_{E\sigma} \\ \mathbb{F}_{ES} & \frac{14}{9}\mathbb{F}_{\gamma s} & \frac{14}{9}\mathbb{F}_{\gamma \sigma} \\ \mathbb{F}_{E\sigma} & \frac{14}{9}\mathbb{F}_{\gamma \sigma} & \frac{14}{9}\mathbb{F}_{\gamma \sigma} \end{bmatrix} \begin{Bmatrix} N_2 \\ T_2 \\ \Sigma_2 \end{Bmatrix}$$

$$\begin{Bmatrix} \hat{E}_3 \\ \gamma_3 \\ \epsilon_3 \end{Bmatrix} = \frac{\sqrt{21}}{11}\begin{bmatrix} 0 & 0 & 0 \\ 0 & \mathbb{F}_{\gamma s} & \mathbb{F}_{\gamma \sigma} \\ 0 & \mathbb{F}_{\gamma \sigma} & \mathbb{F}_{\epsilon \sigma} \end{bmatrix} \begin{Bmatrix} N_1 \\ T_1 \\ \Sigma_1 \end{Bmatrix}$$

$$+ \begin{bmatrix} \mathbb{F}_{ES} & \mathbb{F}_{Es} & \mathbb{F}_{E\sigma} \\ \mathbb{F}_{ES} & \frac{18}{11}\mathbb{F}_{\gamma s} & \frac{18}{11}\mathbb{F}_{\gamma \sigma} \\ \mathbb{F}_{E\sigma} & \frac{18}{11}\mathbb{F}_{\gamma \sigma} & \frac{18}{11}\mathbb{F}_{\epsilon \sigma} \end{bmatrix} \begin{Bmatrix} N_3 \\ T_3 \\ \Sigma_3 \end{Bmatrix} \qquad (37)$$

The strain–displacement relations (13a–13c) become

$$\hat{E}_i = v_i', \qquad \gamma_i = (D_{ji}v_j + w_i')/2, \qquad \epsilon_i = D_{ji}w_j \quad (38)$$

Substitution from Eq. (38) into Eq. (37); solving the resulting equations for N_i, T_i, and Σ_i; and substitution for N_i, T_i, and Σ_i into Eq. (35) gives a set of coupled linear second-order ordinary differential equations in v_i and w_i that can be solved under the boundary conditions (36).

The aforestated boundary-value problem for a graphite–epoxy beam with $\mathbb{F}_{ES} = 55.25$, $\mathbb{F}_{Es} = 0$, $\mathbb{F}_{E\sigma} = -15.47$, $\mathbb{F}_{\gamma s} = 3484.3$, $\mathbb{F}_{\gamma \sigma} = 0$, and $\mathbb{F}_{\epsilon \sigma} = 970.92(1/10^{13})$ Pa) is analyzed by the finite element method by using piecewise linear basis functions. The domain $[0, L]$ is divided into 50 uniform elements, the element matrices and the load vector are evaluated exactly by integrating their expressions with Mathematica, and the essential boundary conditions are applied by the penalty method. There are $2(K + 1)$ unknowns, $v_0, v_1, \ldots, v_K$ and $w_0, w_1, \ldots, w_K$, at each node; thus, the number
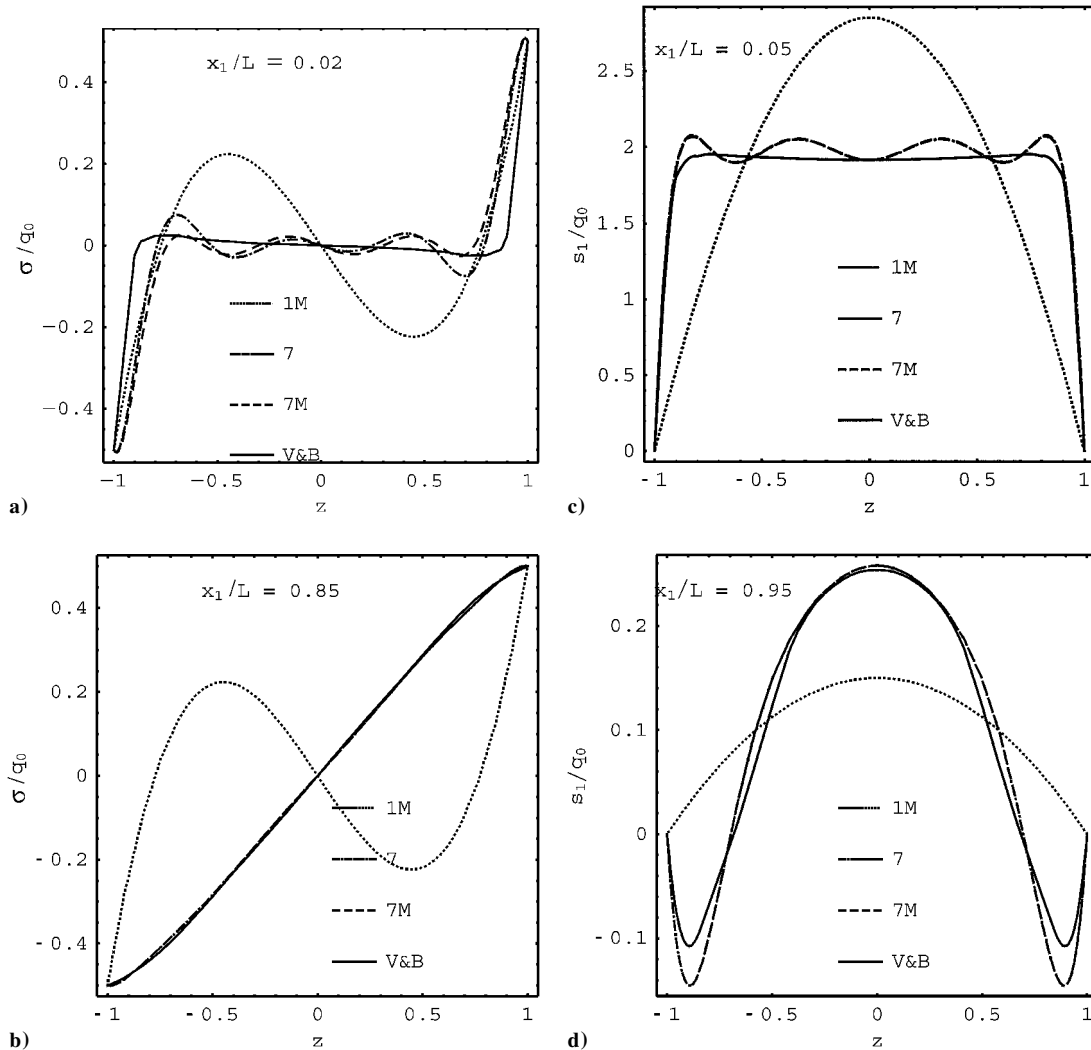
Fig. 1   Through-the-thickness variation on sections of a thick cantilevered beam: a) and b) transverse normal stress and c) and d) transverse shear stress.

of degrees of freedom equals $102(K + 1)$. On the Pentium II laptop computer, it took approximately 2 min to solve the problem for $K = 7$ and 3 s for $K = 1$. Results computed with 100 elements were virtually indistinguishable from those for 50 elements.

Figures 1a–1d depict through-the-thickness variation of the transverse normal stress, σ, on the sections $x_1/L = 0.02$ and 0.85 and of the transverse shear stress s_1 on the sections $x_1/L = 0.05$ and 0.95 computed with the present plate theory by setting $K = 1$ and 7; analytical results (identified as V&B in Fig. 1) of Vel and Batra[22] are also plotted for comparison purposes. Results were also computed for $K = 0, 1, 2, \ldots, 7$, but only those for $K = 1$ and 7 are shown so as not to clutter the plots. Results obtained with the modified constitutive relation (31) for $K = 7$ are identified by $7M$, and those computed with the constitutive relation (22) are signified without the M. It is clear that the seventh-order plate theory gives results that agree well with the analytical solution, and the amplitude of oscillations for the results computed with the constitutive relation (31) is smaller than that obtained with the constitutive relation (22). Stresses computed from the first-order, that is, for $K = 1$, theory do not agree even qualitatively with the analytical solution. A good agreement with the analytical results at sections close to the clamped edge and the free edge indicates that the seventh-order plate theory captures well the through-the-thickness distribution of the transverse normal and the transverse shear stresses near the clamped and the free edges. In Fig. 1b, results computed with the plate theories 7 and $7M$ essentially coincide with each other. However, in Figs. 1c and 1d, these two sets of results overlap each other because s_1 vanishes on the top and the bottom surfaces of the plate. The distribution of the longitudinal stress $\hat{S}_{11}$ on horizontal planes $z = 0.9, 0.75, 0.5$, and

0.25 plotted in Fig. 2a depicts the boundary-layer effect near the clamped edge. On all four horizontal planes, $\hat{S}_{11}$ nearly vanishes at $x_1/L = 1$, signifying that the natural boundary conditions at the free edge are well satisfied. In the Euler beam theory $\hat{S}_{11}$ is independent of x_1, and the boundary condition of zero tractions at the edge $x_1 = L$ is satisfied in the mean. Here we require that the moments of $\hat{S}_{11}$ up to order 7 vanish on the surface $x_1 = L$. Figures 2b and 2c exhibit through-the-thickness distribution of the normalized longitudinal stress, $\hat{S}_{11}/q_0$, on the sections $x_1/L = 0.4$ and 0.85, respectively. Whereas on the section $x_1/L = 0.4$ the variation of $\hat{S}_{11}$ may be approximated as affine, on the plane $x_1/L = 0.85$ it exhibits boundary layers near the top and the bottom surfaces. The through-the-thickness variation of $\hat{S}_{11}/q_0$ near the free edge $x_1/L = 0.85$ computed with the plate theory $7M$ is in good agreement with the analytical solution of Vel and Batra.[22] The deflected shapes of the top surface plotted in Fig. 2d suggest that the first-order theory gives acceptable values of the deformed shape. In Figs. 2b and 2c, the two plate theories 7 and $7M$ give identical results because the expansions for $\hat{S}$ are the same in the two theories. The variation with K of the total strain energies of bending, transverse shear, and transverse extensional deformations normalized with respect to their respective values for $K = 7$ is plotted in Fig. 3; these are denoted by E_1, E_2, and E_3, respectively. It is clear that the fourth-order plate theory gives acceptable values of the three energies. However, for $K = 4$, the through-the-thickness variation of the transverse shear and the transverse normal stresses did not match well with the analytical results. Thus, the total strain energy of the beam is not a good indicator of the quality of the solution within the beam. The first-order plate theory overestimates the total
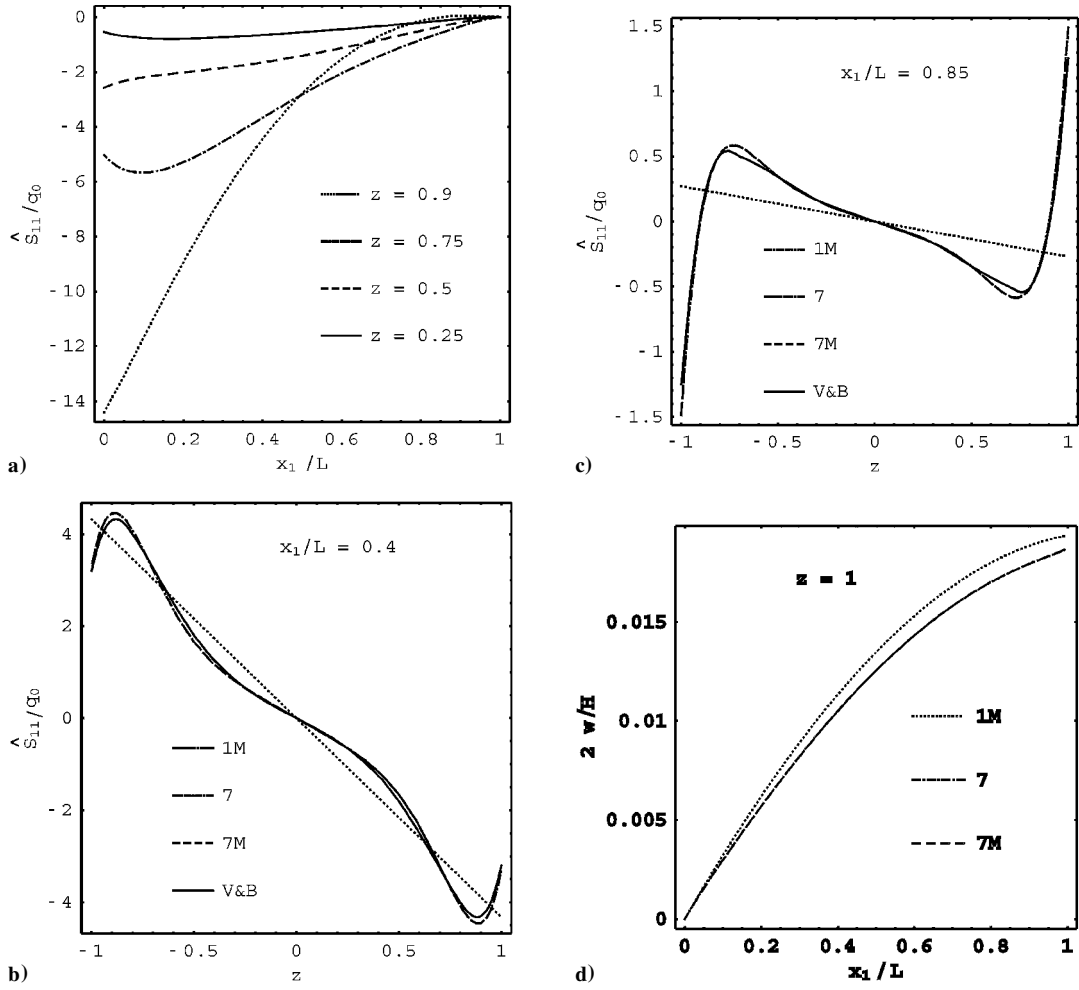
Fig. 2   Normalized longitudinal stress: a) distribution on horizontal planes of a thick cantilever beam and b) and c) through-the-thickness distribution. Panel d shows the deflected shape of the top surface of a thick cantilever beam.
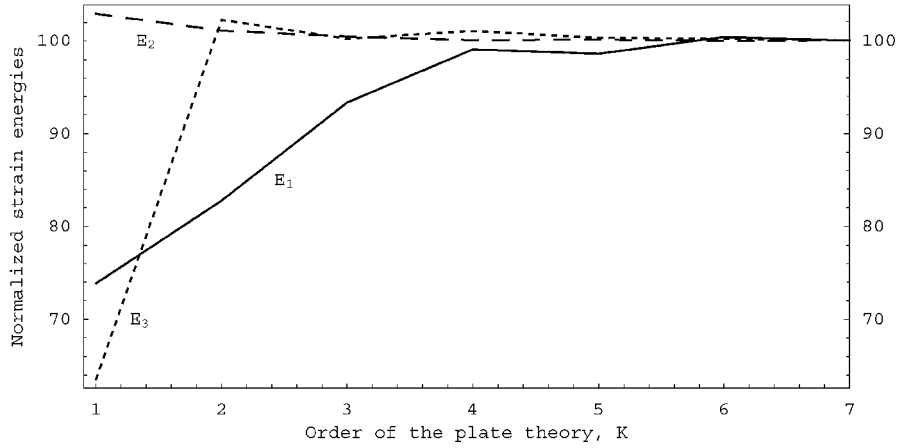
Fig. 3   Dependence of the normalized total strain energies of bending, transverse shear, and transverse extensional deformations of a thick cantilever beam on the order of the plate theory.

strain energy of the transverse shear deformations and underestimates the total strain energy of bending and transverse extensional deformations.

For the cantilever beam loaded with a uniformly distributed pressure load applied to the top surface only, Fig. 4 exhibits the variation of W_1, W_2, and W_3 with the span to thickness ratio L/H. Here W_1, W_2, and W_3 equal, respectively, the total strain energy

$$\frac{1}{2}\int_{\mathcal{C}}\mathrm{tr}(\hat{\boldsymbol{S}}\hat{\boldsymbol{E}}^T)$$

of bending, transverse shear

$$\int_{\mathcal{C}}\boldsymbol{s}\cdot\boldsymbol{\gamma}$$

and transverse extensional

$$\frac{1}{2}\int_{\mathcal{C}}\sigma\epsilon$$

deformations of the beam. These have been normalized with respect to the total energy, $W_1 + W_2 + W_3$, of the beam and have been computed for $K = 7$ with the constitutive relation (31). For the beam loaded by a uniformly distributed pressure on the top surface, W_3 is small and has noticeable values only for $L/H \leq 5$. However, the
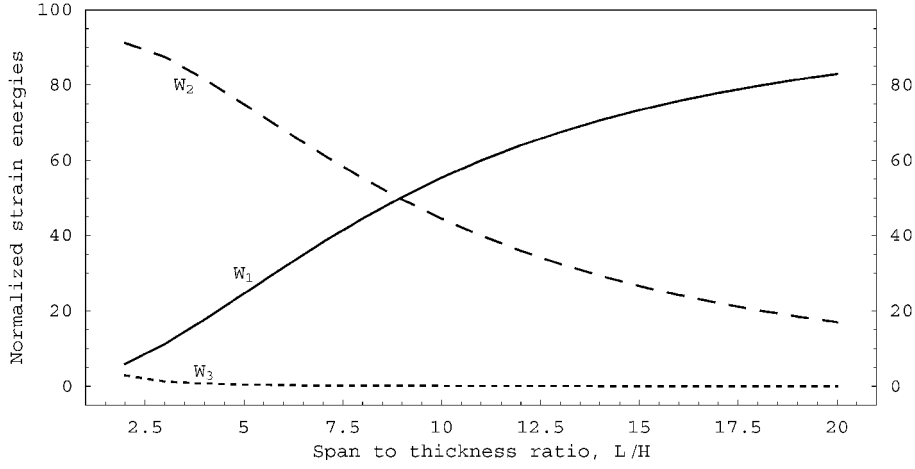
Fig. 4 Variation with the span to the thickness ratio of the total strain energy due to bending, transverse shearing, and transverse extensional deformations of a cantilever beam loaded by a uniformly distributed pressure on the top surface.

strain energy of transverse shear deformations equals 15% of the total strain energy of the beam even when $L/H = 20$. Recall that the beam is orthotropic.

Numerical results for the following three example problems have been computed with the seventh-order plate theory by using the constitutive relation (31).

2. Cantilever Thick Beam Loaded by Equal and Opposite Uniformly Distributed Tangential Tractions on Its Top and Bottom Surfaces

We now consider the case when the top and the bottom surfaces of the cantilever beam are loaded by uniformly distributed equal and opposite tangential tractions $(p_0/2)\delta_{i1}$ and $(-p_0/2)\delta_{i1}$, respectively. For the third-order beam theory, the balance laws (17) simplify to

$$N_0' = 0, \qquad T_0' = 0, \qquad N_1' - \sqrt{3}T_0 + \sqrt{\tfrac{3}{2}}p_0 = 0$$

$$T_1' - \sqrt{3}\Sigma_0 = 0, \qquad N_2' - \sqrt{15}T_1 = 0, \qquad T_2' - \sqrt{15}\Sigma_1 = 0$$

$$N_3' - \sqrt{7}T_0 - \sqrt{35}T_2 + \sqrt{\tfrac{7}{2}}p_0 = 0$$

$$T_3' - \sqrt{7}\Sigma_0 - \sqrt{35}\Sigma_2 = 0, \qquad 0 < x_1 < L \qquad (39)$$

Boundary conditions (36), and the strain–displacement relations (38) are still valid. However, constitutive relations (37) are replaced by

$$
\begin{Bmatrix} \hat{E}_i \\ \gamma_i \\ \epsilon_i \end{Bmatrix}
=
\begin{bmatrix}
\mathbb{F}_{ES}\delta_{ij} & \mathbb{F}_{Es} & \mathbb{F}_{E\sigma}\delta_{ij} \\
* & \mathbb{F}_{\gamma s}P_{ij} & \mathbb{F}_{\gamma\sigma}P_{ij} \\
* & * & \mathbb{F}_{\epsilon\sigma}P_{ij}
\end{bmatrix}
\begin{Bmatrix} N_j \\ T_j \\ \Sigma_j \end{Bmatrix}
$$

$$
+ \delta_{io}\left(-\frac{\sqrt{2}}{18}p_0\right)
\begin{Bmatrix} 0 \\ \mathbb{F}_{\gamma s} \\ \mathbb{F}_{\gamma\sigma} \end{Bmatrix}
\qquad (40)
$$

Note that γ_3 depends on T_1, T_3, Σ_1, and Σ_3 provided that $\mathbb{F}_{\gamma s}$ and $\mathbb{F}_{\gamma\sigma}$ are nonzero.

Figure 5a exhibits the deformed shape of the graphite-epoxy cantilever beam with the span to thickness ratio of two. It is clear that a normal to the midsurface is severely deformed, especially at points close to the top and the bottom surfaces of the beam, signifying large shear deformations there. The variation of the normalized total strain energies associated with the bending, transverse shear, and transverse extensional deformations with the span to the thickness ratio L/H is depicted in Fig. 5b. Unlike the case of the cantilever beam loaded by a uniformly distributed pressure on the top surface, the fraction of the strain energy due to transverse shearing deformation is negligible for $L/H \geq 10$. Recall that in the earlier case it equaled 15% of the total strain energy even when $L/H = 20$. In Figs. 5c and 5d, we have plotted through-the-thickness variation of the transverse shear stress and the transverse normal stress on the four cross sections, $x_1/L = 0.05, 0.6, 0.8$, and 0.95. The transverse

shear stress has sharp gradients and, hence, exhibits boundary layers near the top and the bottom surfaces of the beam where tangential tractions are applied. Except for points near the free edge of the cantilever beam, the transverse normal stresses are quite small and usually less than 7% of the applied tangential tractions. However, the magnitude of the maximum transverse shear stress occurs at points on the top and the bottom surfaces of the beam. In the Euler beam theory the loading considered herein will be replaced by uniformly distributed moments along the span of the beam. In some of the higher-order plate theories[14,15] the transverse shear strain and, hence, the transverse shear stress is required to vanish on the top and the bottom surfaces of the plate. Such theories are tacitly meant to analyze plates subjected to pressure loads on the top and the bottom surfaces and will need to be modified to get very good answers for the present problem.

B. Deformations of a PZT Plate
1. Cantilever Thick Beam Loaded by Uniformly Distributed Charge Density on Its Top and Bottom Surfaces

The electromechanical deformations of a cantilever beam made of a PZT5A ceramic and the span to thickness ratio of two are studied. The axis of polarization and, hence, of transverse isotropy is along the thickness direction. The load consists of a uniform charge density of $c_0/2$ on the top surface and $(-c_0/2)$ on the bottom surface of the plate. The balance laws (17a) and (17b) reduce to Eqs. (39) with $p_0 = 0$, and the balance law (17c) takes the form

$$\Delta_0' = 0, \qquad \Delta_1' - \sqrt{3}d_0 + \sqrt{\tfrac{3}{2}}c_0 = 0, \qquad \Delta_2' - \sqrt{15}d_1 = 0$$

$$\Delta_3' - \sqrt{7}d_0 - \sqrt{35}d_2 + \sqrt{\tfrac{7}{2}}c_0 = 0, \qquad 0 < x_1 < L \quad (41)$$

The boundary conditions (36) are supplemented by

$$\varphi_0 = \varphi_1 = \varphi_2 = \varphi_3 = 0 \quad \text{at} \quad x_1 = 0$$

$$\Delta_0 = \Delta_1 = \Delta_2 = \Delta_3 = 0 \quad \text{at} \quad x_1 = L \qquad (42)$$

and the constitutive relations (31) become

$$
\begin{Bmatrix} \hat{E}_i \\ \gamma_i \\ \epsilon_i \\ \hat{W}_i \\ \omega_i \end{Bmatrix}
=
\begin{bmatrix}
\mathbb{F}_{ES}\delta_{ij} & \mathbb{F}_{Es}\delta_{ij} & \mathbb{F}_{E\sigma}\delta_{ij} & \mathbb{M}_{ED}\delta_{ij} & \mathbb{M}_{E\delta}\delta_{ij} \\
\mathbb{F}_{Es}P_{ij} & \mathbb{F}_{\gamma s}P_{ij} & \mathbb{F}_{\gamma\sigma}P_{ij} & \mathbb{M}_{\gamma D}\delta_{ij} & \mathbb{M}_{\gamma\delta}P_{ij} \\
\mathbb{F}_{E\sigma}\delta_{ij} & \mathbb{F}_{\gamma\sigma}P_{ji} & \mathbb{F}_{\epsilon\sigma}P_{ij} & \mathbb{M}_{\epsilon D}\delta_{ij} & \mathbb{M}_{\epsilon\delta}P_{ij} \\
\mathbb{M}_{ED}\delta_{ij} & \mathbb{M}_{\gamma D}\delta_{ij} & \mathbb{M}_{\epsilon D}\delta_{ij} & \mathbb{N}_{WD}\delta_{ij} & \mathbb{N}_{W\delta}\delta_{ij} \\
\mathbb{M}_{E\delta}\delta_{ij} & \mathbb{M}_{\gamma\delta}P_{ij} & \mathbb{M}_{\epsilon\delta}P_{ij} & \mathbb{N}_{W\delta}\delta_{ij} & \mathbb{N}_{\omega\delta}P_{ij}
\end{bmatrix}
$$

$$
\times
\begin{Bmatrix} N_j \\ T_j \\ \Sigma_j \\ \Delta_j \\ d_j \end{Bmatrix}
+ \left(-\frac{\sqrt{2}}{18}c_0\right)\delta_{i0}
\begin{Bmatrix} 0 \\ \mathbb{M}_{\gamma\delta} \\ \mathbb{M}_{\epsilon\delta} \\ 0 \\ \mathbb{N}_{W\delta} \end{Bmatrix}
\qquad (43)
$$
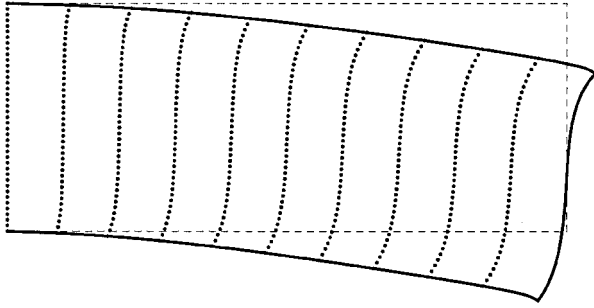
Fig. 5a Deformed shape of a thick cantilever beam loaded by uniformly distributed tangential tractions on its top and bottom surfaces.
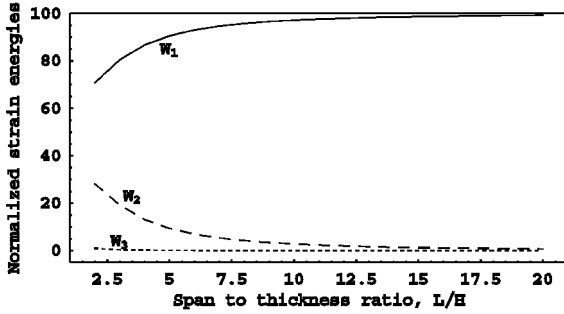
Fig. 5b Variation with the span to thickness ratio of the normalized total strain energies due to the bending, transverse shear, and transverse extensional deformations of a beam loaded by equal and opposite uniformly distributed tangential tractions on its top and bottom surfaces.
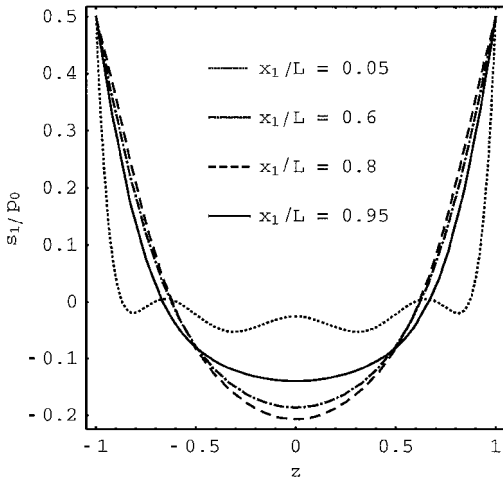
Fig. 5c Through-the-thickness variation of the transverse shear stresses on four cross sections.
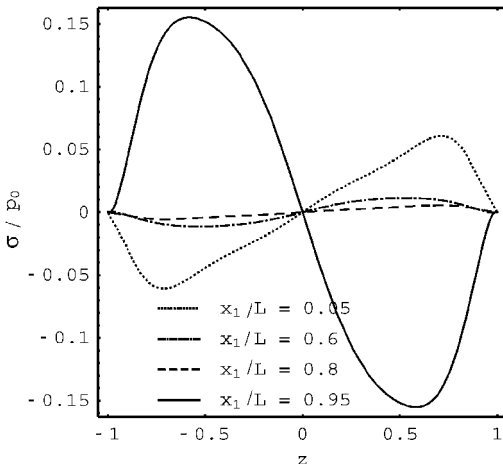
Fig. 5d Through-the-thickness variation of the transverse normal stresses on four cross sections.

In addition to the strain–displacement relations (38), we have

$$\hat{W}_i = -\varphi_i', \qquad \omega_i = -D_{ji}\varphi_j \tag{44}$$

Substitution from Eqs. (43), (38), and (44) into the balance laws (39) with $p_0 = 0$ and Eqs. (41) yields a set of coupled linear second-order ordinary differential equations in v_i, w_i, and φ_i. These are solved by the finite element method as described earlier. In the solution of the problem, the material parameters were assigned the following values:

$$\mathbb{F}_{ES} = 127.92, \qquad \mathbb{F}_{Es} = 0, \qquad \mathbb{F}_{E\sigma} = 16.47$$

$$\mathbb{F}_{\gamma s} = 191.92, \qquad \mathbb{F}_{\gamma\sigma} = 0, \qquad \mathbb{F}_{\epsilon\sigma} = 399.53(1/10^{13}\,\text{Pa})$$

$$\mathbb{M}_{ED} = 0, \qquad \mathbb{M}_{E\delta} = -210.6, \qquad \mathbb{M}_{\gamma D} = 0, \qquad \mathbb{M}_{\gamma\delta} = 0$$

$$\mathbb{M}_{\epsilon\delta} = 460.61, \qquad \mathbb{M}_{\epsilon D} = 0(\text{m}^2/10^6\,\text{C}), \qquad \mathbb{N}_{WD} = -13.9$$

$$\mathbb{N}_{W\delta} = 0, \qquad \mathbb{N}_{\omega\delta} = -12.32(\text{m}^2/10^3\text{VC})$$

From the deformed shape of the beam plotted in Fig. 6a, it is clear that its deformations are symmetric about the midsurface $z = 0$. The thickness of the beam, except at sections near the clamped edge, increases, and its length decreases. The variation of N_0, N_2, N_4, and N_6 (N_i, $i = 1, 3, 5, 7$ identically vanish) along the span of the beam exhibited in Fig. 6b suggests that boundary condition $\hat{S}_{11} = 0$ at the free edge is well satisfied. Also, there is a boundary-layer effect near the clamped edge. Recall that N_0 is the membranal stress tensor, and $N_i(i > 0)$ equals the linear combination of the moments of $\hat{S}_{11}$ of order 0–i. The through-the-thickness distributions of the transverse normal stress at four sections, $x_1/L = 0.05, 0.1, 0.5$, and 0.75 and of the electric potential on sections $x_1/L = 0.05, 0.1, 0.15$, and 0.5 are exhibited in Figs. 6c and 6d, respectively. The through-the-thickness variation of the transverse normal stress at sections for which $x_1/L \geq 0.75$ is essentially the same. Note that on the section $x_1/L = 0.05$ (i.e., near the clamped edge), the curvature near the top and the bottom surfaces of the curve giving the through-the-thickness distribution of the transverse normal stress is opposite to that at the midspan of the beam. However, the through-the-thickness variation of the electric potential at each section is similar, suggesting that the electric potential does not exhibit any boundary-layer effect near the clamped and the free edges of the thick beam.

2. Cantilever Thick Beam Loaded by Equal and Opposite Normal Tractions on a Part of the Beam

The final example problem involves the investigation of the electromechanical deformations of a cantilever thick beam with the span to thickness ratio of two and loaded by uniformly distributed equal and opposite compressive normal tractions $q_0/2$ applied only to a quarter of the beam ending at its free edge. For this case, the balance laws (17) simplify to

$$N_0' = 0, \qquad T_0' = 0, \qquad \Delta_0' = 0, \qquad N_1' - \sqrt{3}T_0 = 0$$

$$T_1' - \sqrt{3}\Sigma_0 + \sqrt{\tfrac{3}{2}}q_0 H(x - 3L/4) = 0, \qquad \Delta_1' - \sqrt{3}d_0 = 0$$

$$N_2' - \sqrt{15}T_1 = 0, \qquad T_2' - \sqrt{15}\Sigma_1 = 0, \qquad \Delta_2' - \sqrt{15}d_1 = 0$$

$$N_3' - \sqrt{7}T_0 - \sqrt{35}T_2 = 0$$

$$T_3' - \sqrt{7}\Sigma_0 - \sqrt{35}\Sigma_2 + \sqrt{\tfrac{7}{2}}q_0 H(x - 3L/4) = 0$$

$$\Delta_3' - \sqrt{7}d_0 - \sqrt{35}d_2 = 0 \tag{45}$$

where $H(\cdot)$ is the Heaviside step function. Boundary conditions are given by Eqs. (36) and (42), and the constitutive relations are Eqs. (43) with the second term on the right-hand side replaced by $(-\sqrt{2}q_0/18)\delta_{i0}[0\ \mathbb{F}_{\gamma\sigma}\ \mathbb{F}_{\epsilon\sigma}\ 0\ \mathbb{M}_{\epsilon\delta}]^T H(x - 3L/4)$.

From the deformed shape of the beam shown in Fig. 7a, one can conclude that the free edge of the beam is severely deformed, and the deformations of the beam are essentially concentrated in the loaded region. As plotted in Fig. 7b, for $q_0 = 10^7$ N/m^2, the maximum electric potential induced equals ± 2 mV with the negative value occurring at a point on the bottom surface. The electric potential essentially vanishes for $x_1/L \leq 0.5$. The fringe plots of the
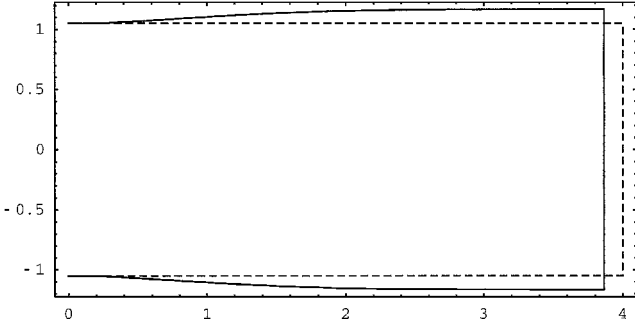
Fig. 6a   Deformed shape of a cantilever thick PZT beam subjected to equal and opposite uniformly distributed charge density on the top and bottom surfaces.
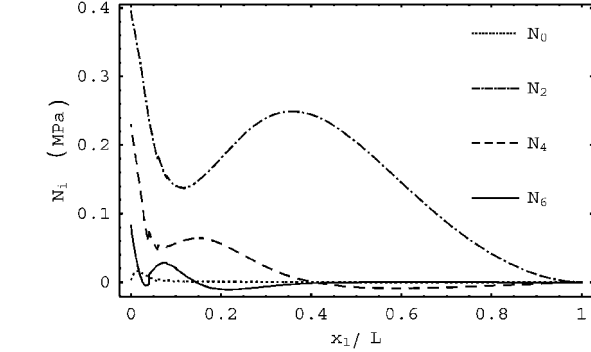
Fig. 6b   Variation of N_0, N_2, N_4, and N_6 along the span of the PZT beam.
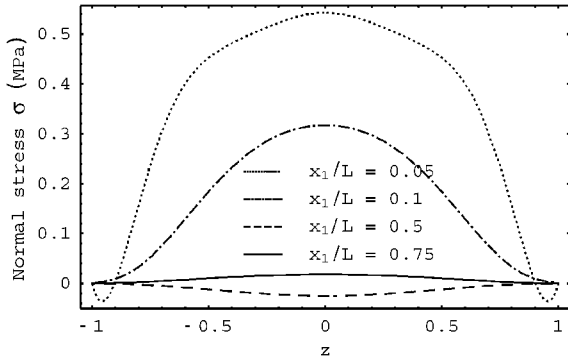
Fig. 6c   Through-the-thickness variations of the transverse normal stress at four sections.
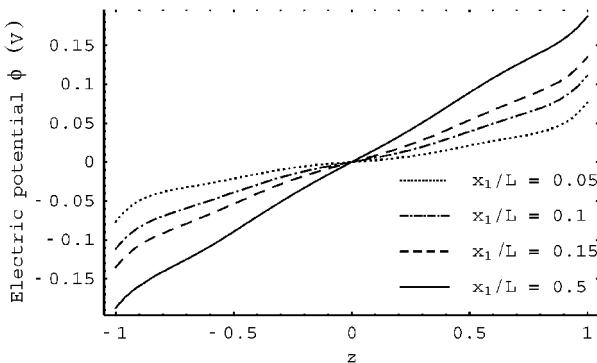
Fig. 6d   Through-the-thickness variations of the electric potential at four sections.

transverse shear stress, depicted in Fig. 7c, reveal that the magnitude of the transverse shear stress is maximum at points on the bounding surfaces of the beam just where the applied distributed load ends. On the front face of the beam, regions of large transverse shear stress are centered around the extremity of the applied load. Figure 7d exhibits the distribution of the transverse normal stress on four horizontal planes, namely, $z = 0.75$, 0.9, 0.95, and 1. The distribution of the transverse normal stress on the top surface exactly matches
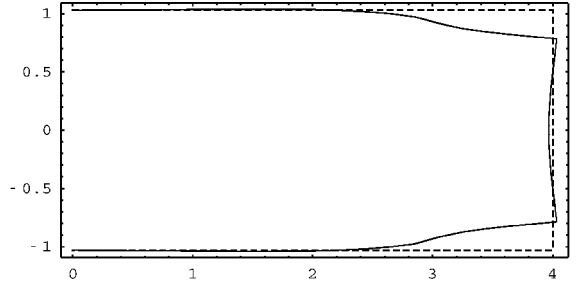
Fig. 7a   Deformed shape of a thick cantilever PZT beam loaded on a quarter of its length starting from the free edge by equal and opposite uniformly distributed normal tractions.
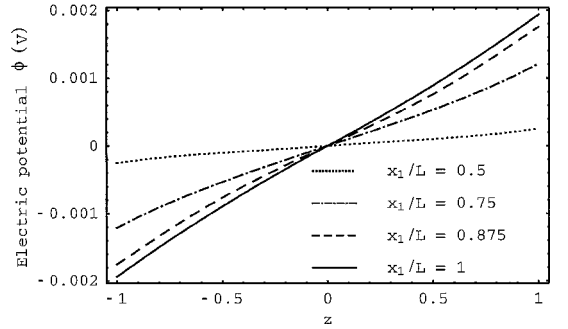
Fig. 7b   Distribution of the electric potential on four sections of the thick cantilever PZT beam.
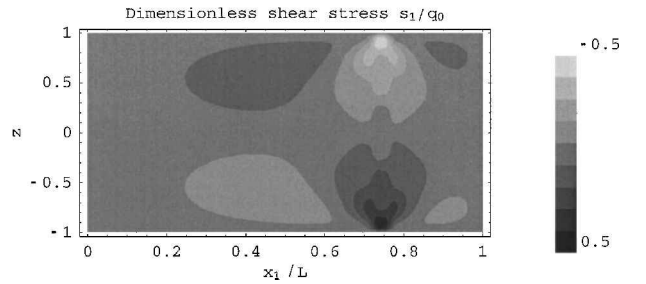
Fig. 7c   Fringe plots of the transverse shear stress in the thick cantilever PZT beam.
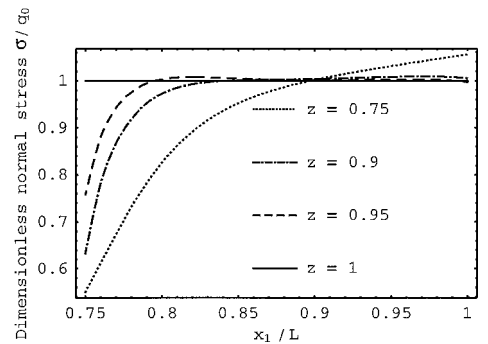
Fig. 7d   Distribution of the transverse normal stress on four horizontal planes of the thick cantilever PZT beam.

with that of the applied normal traction, signifying that the boundary conditions are well satisfied. The discontinuity in the applied normal traction propagates through the thickness of the beam up to a distance of about a quarter of the beam's thickness. Also, the magnitude of the maximum transverse normal stress at points near the free edge and lying on the surface $z = 0.75$ exceeds that of the normal tractions applied on the surface $z = 1$.

V.   Conclusions

By using the three-dimensional mixed variational principle of Yang and Batra,[19] we have derived a higher-order PZT plate theory. The electric potential and the three components of the mechanical displacement are expanded in the thickness coordinate z up to terms of order K by taking normalized Legendre polynomials $L_i(z)$ as

the basis functions. The normal and the tangential tractions and the charge density applied to the top and the bottom surfaces of the plate are incorporated in the theory. The in-plane components of the stress tensor and the electric field are also expressed as a finite series in z upto terms involving z^K. However, the series expansions of the transverse shear stress, the transverse normal stress, and the transverse electric displacement contain terms of order $K + 2$. The boundary conditions on the top and the bottom surfaces of the plate are exactly satisfied. The distributions of the transverse shear and the transverse normal stresses in a cantilever thick beam with the span to thickness ratio of two and computed with $K = 7$ match well with the analytical solutions of Vel and Batra.[22] This seventh-order theory also captures well the boundary-layer effects near the clamped and the free edges of the beam, and also adjacent to its top and the bottom surfaces.

The equilibrium equations involve second-order derivatives of the in-plane, v_i, and transverse, w_i, mechanical displacements and the electric potential ϕ_i. The index i signifies the order of the plate theory, or, equivalently, the term multiplying $L_i(z)$ in the series expansion. Thus, lower-order finite elements can be used to solve the problem numerically. We note that equilibrium equations for v_K, w_K, and ϕ_K may involve all terms of order less than K; thus, equations are strongly coupled.

The plate theory has been used to numerically solve four problems for an orthotropic cantilever thick beam of span to thickness ratio of two. The two mechanical problems involve either uniformly distributed normal or tangential tractions on the top and the bottom surfaces of the beam. In each case the total strain energy density converges for $K = 4$, and the computed deflected shape is reasonably good for $K = 1$. However, the boundary-layer effects near the loaded surfaces are captured well for $K = 7$. For the cantilever beam loaded by uniformly distributed normal tractions on the top surface, the total strain energy due to transverse extensional deformations is a significant part of the total strain energy for the span to thickness ratio $(L/H) \leq 4$. For $L/H \geq 10$, the strain energy due to bending deformations predominates that due to transverse extensional and transverse shearing deformations. For $L/H = 20$, the strain energy due to transverse shearing deformations equals approximately 15% of the total strain energy.

Results have also been computed for a cantilever thick PZT beam loaded on a quarter of its length, starting with the free edge, by equal and opposite normal tractions. It is found that the induced electric potential is nonzero in only one-half of the beam, and the maximum transverse shear stress occurs at points of the beam underneath the extremities of the applied load. For the PZT beam loaded by equal and opposite uniformly distributed charge density on the top and the bottom surfaces, the through-the-thickness distribution of the transverse normal stress on the section close to the clamped edge exhibits boundary-layer effects near the loaded surfaces. Its curvature near the top and the bottom surfaces of the beam is opposite to that at the midplane.

The CPU time required to compute results for the seventh-order beam theory is negligible (less than 0.1%) as compared to that for the analytical series solution of Vel and Batra.[22] Also, the total effort required to analyze a thick beam problem is considerably less than that needed to solve the same problem by the finite element method.

Batra et al.[21] have analyzed plane traveling waves and frequencies of free vibrations of a simply supported plate. Frequencies computed with the fifth-order plate theory are found to match extremely well with those computed from the three-dimensional elasticity theory.

Appendix: Expressions for Variables Appearing in the Seventh-Order Plate Theory

Legendre polynomials, normalized according to Eq. (9), of degree 4–7, are

$$L_4 = \frac{3}{\sqrt{2}}\left(\frac{3}{8} - \frac{15z^2}{4} + \frac{35z^4}{8}\right)$$

$$L_5 = \sqrt{\frac{11}{2}}\left(\frac{15z}{8} - \frac{35z^3}{4} + \frac{63z^5}{8}\right)$$

$$L_6 = \sqrt{\frac{13}{2}}\left(-\frac{5}{16} + \frac{105z^2}{16} - \frac{315z^4}{16} + \frac{231z^6}{16}\right)$$

$$L_7 = \sqrt{\frac{15}{2}}\left(\frac{-35z}{16} + \frac{315z^3}{16} - \frac{693z^5}{16} + \frac{429z^7}{16}\right) \quad \text{(A1)}$$

For $K = 7$, the matrix D_{ij} introduced in Eq. (12) is given by

$$D = \begin{pmatrix} 0 & 0 & 0 & 0 & 0 & 0 & 0 & 0 \\ \sqrt{3} & 0 & 0 & 0 & 0 & 0 & 0 & 0 \\ 0 & \sqrt{15} & 0 & 0 & 0 & 0 & 0 & 0 \\ \sqrt{7} & 0 & \sqrt{35} & 0 & 0 & 0 & 0 & 0 \\ 0 & 3\sqrt{3} & 0 & 3\sqrt{7} & 0 & 0 & 0 & 0 \\ \sqrt{11} & 0 & \sqrt{55} & 0 & 3\sqrt{13} & 0 & 0 & 0 \\ 0 & \sqrt{39} & 0 & \sqrt{91} & 0 & \sqrt{143} & 0 & 0 \\ \sqrt{15} & 0 & 5\sqrt{3} & 0 & 3\sqrt{15} & 0 & \sqrt{195} & 0 \end{pmatrix}$$

$$\text{(A2)}$$

We denote by $\tilde{B}$ the set of $(K + 1)$ functions $\tilde{L}_0(z)$, $\tilde{L}_1(z)$, $\tilde{L}_2(z), \ldots, \tilde{L}_K(z)$, defined by Eqs. (21a) and (21b). Recalling that P_{ij} is defined by Eq. (24a), we list hereafter the functions in $\tilde{B}$ and the matrices P_{ij} for different values of K, except for $K = 3$, for which these are given in the text.

For $K = 1$,

$$\tilde{B} = \left\{ \sqrt{2}\left(\frac{3}{4} - \frac{3z^2}{4}\right), \sqrt{\frac{2}{3}}\left(\frac{15z}{4} - \frac{15z^3}{4}\right) \right\} \quad \text{(A3)}$$

$$P = \begin{pmatrix} \frac{6}{5} & 0 \\ 0 & \frac{10}{7} \end{pmatrix} \quad \text{(A4)}$$

For $K = 2$,

$$\tilde{B} = \left\{ \begin{array}{c} \sqrt{2}\left(\frac{5}{16} + \frac{15z^2}{8} - \frac{35z^4}{16}\right), \sqrt{\frac{2}{3}}\left(\frac{15z}{4} - \frac{15z^3}{4}\right) \\ \sqrt{\frac{2}{5}}\left(-\frac{35}{16} + \frac{105z^2}{8} - \frac{175z^4}{16}\right) \end{array} \right\} \quad \text{(A5)}$$

$$P = \begin{pmatrix} \frac{10}{9} & 0 & \frac{\sqrt{5}}{9} \\ 0 & \frac{10}{7} & 0 \\ \frac{\sqrt{5}}{9} & 0 & \frac{14}{9} \end{pmatrix} \quad \text{(A6)}$$

For $K = 4$,

$$\tilde{B} = \left\{ \begin{array}{c} \sqrt{2}\left(\frac{21}{32} - \frac{105z^2}{32} + \frac{315z^4}{32} - \frac{231z^6}{32}\right) \\ \sqrt{\frac{2}{3}}\left(\frac{-21z}{16} + \frac{105z^3}{8} - \frac{189z^5}{16}\right) \\ \sqrt{\frac{2}{5}}\left(-\frac{15}{32} - \frac{405z^2}{32} + \frac{1575z^4}{32} - \frac{1155z^6}{32}\right) \\ \sqrt{\frac{2}{7}}\left(\frac{-189z}{16} + \frac{315z^3}{8} - \frac{441z^5}{16}\right) \\ \frac{\sqrt{2}}{3}\left(\frac{99}{32} - \frac{1485z^2}{32} + \frac{3465z^4}{32} - \frac{2079z^6}{32}\right) \end{array} \right\} \quad \text{(A7)}$$

$$P = \begin{pmatrix} \dfrac{14}{13} & 0 & \dfrac{\sqrt{5}}{13} & 0 & \dfrac{3}{13} \\[2mm] 0 & \dfrac{14}{11} & 0 & \dfrac{\sqrt{21}}{11} & 0 \\[2mm] \dfrac{\sqrt{5}}{13} & 0 & \dfrac{18}{13} & 0 & \dfrac{3\sqrt{5}}{13} \\[2mm] 0 & \dfrac{\sqrt{21}}{11} & 0 & \dfrac{18}{11} & 0 \\[2mm] \dfrac{3}{13} & 0 & \dfrac{3\sqrt{5}}{13} & 0 & \dfrac{22}{13} \end{pmatrix} \quad (A8)$$

For $K = 5$,

$$\tilde{B} = \begin{Bmatrix} \sqrt{2}\left(\dfrac{21}{32} - \dfrac{105z^2}{32} + \dfrac{315z^4}{32} - \dfrac{231z^6}{32}\right) \\[2mm] \sqrt{\dfrac{2}{3}}\left(\dfrac{153z}{32} - \dfrac{945z^3}{32} + \dfrac{2079z^5}{32} - \dfrac{1287z^7}{32}\right) \\[2mm] \sqrt{\dfrac{2}{5}}\left(-\dfrac{15}{32} - \dfrac{405z^2}{32} + \dfrac{1575z^4}{32} - \dfrac{1155z^6}{32}\right) \\[2mm] \sqrt{\dfrac{2}{7}}\left(\dfrac{77z}{32} - \dfrac{1925z^3}{32} + \dfrac{4851z^5}{32} - \dfrac{3003z^7}{32}\right) \\[2mm] \dfrac{\sqrt{2}}{3}\left(\dfrac{99}{32} - \dfrac{1485z^2}{32} + \dfrac{3465z^4}{32} - \dfrac{2079z^6}{32}\right) \\[2mm] \sqrt{\dfrac{2}{11}}\left(\dfrac{715z}{32} - \dfrac{5005z^3}{32} + \dfrac{9009z^5}{32} - \dfrac{4719z^7}{32}\right) \end{Bmatrix} \quad (A9)$$

$$P = \begin{pmatrix} \dfrac{14}{13} & 0 & \dfrac{\sqrt{5}}{13} & 0 & \dfrac{3}{13} & 0 \\[2mm] 0 & \dfrac{18}{15} & 0 & \dfrac{\sqrt{21}}{15} & 0 & \dfrac{\sqrt{33}}{15} \\[2mm] \dfrac{\sqrt{5}}{13} & 0 & \dfrac{18}{13} & 0 & \dfrac{3\sqrt{5}}{13} & 0 \\[2mm] 0 & \dfrac{\sqrt{21}}{15} & 0 & \dfrac{22}{15} & 0 & \dfrac{\sqrt{77}}{15} \\[2mm] \dfrac{3}{13} & 0 & \dfrac{3\sqrt{5}}{13} & 0 & \dfrac{22}{13} & 0 \\[2mm] 0 & \dfrac{\sqrt{33}}{15} & 0 & \dfrac{\sqrt{77}}{15} & 0 & \dfrac{26}{15} \end{pmatrix} \quad (A10)$$

For $K = 6$,

$$\tilde{B} = \begin{Bmatrix} \sqrt{2}\left(\dfrac{93}{256} + \dfrac{315z^2}{64} - \dfrac{3465z^4}{128} + \dfrac{3003z^6}{64} - \dfrac{6435z^8}{256}\right) \\[2mm] \sqrt{\dfrac{2}{3}}\left(\dfrac{153z}{32} - \dfrac{945z^3}{32} + \dfrac{2079z^5}{32} - \dfrac{1287z^7}{32}\right) \\[2mm] \sqrt{\dfrac{2}{5}}\left(-\dfrac{495}{256} + \dfrac{1815z^2}{64} - \dfrac{17,325z^4}{128} + \dfrac{15,015z^6}{64} - \dfrac{32,175z^8}{256}\right) \\[2mm] \sqrt{\dfrac{2}{7}}\left(\dfrac{77z}{32} - \dfrac{1925z^3}{32} + \dfrac{4851z^5}{32} - \dfrac{3003z^7}{32}\right) \\[2mm] \dfrac{\sqrt{2}}{3}\left(\dfrac{117}{256} + \dfrac{1755z^2}{64} - \dfrac{28,665z^4}{128} + \dfrac{27,027z^6}{64} - \dfrac{57,915z^8}{256}\right) \\[2mm] \sqrt{\dfrac{2}{11}}\left(\dfrac{715z}{32} - \dfrac{5005z^3}{32} + \dfrac{9009z^5}{32} - \dfrac{4719z^7}{32}\right) \\[2mm] \sqrt{\dfrac{2}{13}}\left(-\dfrac{975}{256} + \dfrac{6825z^2}{64} - \dfrac{61,425z^4}{128} + \dfrac{45,045z^6}{64} - \dfrac{83,655z^8}{256}\right) \end{Bmatrix} \quad (A11)$$

$$P = \begin{pmatrix} \dfrac{18}{17} & 0 & \dfrac{\sqrt{5}}{17} & 0 & \dfrac{3}{17} & 0 & \dfrac{\sqrt{13}}{17} \\[2mm] 0 & \dfrac{18}{15} & 0 & \dfrac{\sqrt{21}}{15} & 0 & \dfrac{\sqrt{33}}{15} & 0 \\[2mm] \dfrac{\sqrt{5}}{17} & 0 & \dfrac{22}{17} & 0 & \dfrac{3\sqrt{5}}{17} & 0 & \dfrac{\sqrt{65}}{17} \\[2mm] 0 & \dfrac{\sqrt{21}}{15} & 0 & \dfrac{22}{15} & 0 & \dfrac{\sqrt{77}}{15} & 0 \\[2mm] \dfrac{3}{17} & 0 & \dfrac{3\sqrt{5}}{17} & 0 & \dfrac{26}{17} & 0 & \dfrac{3\sqrt{13}}{17} \\[2mm] 0 & \dfrac{\sqrt{33}}{15} & 0 & \dfrac{\sqrt{77}}{15} & 0 & \dfrac{26}{15} & 0 \\[2mm] \dfrac{\sqrt{13}}{17} & 0 & \dfrac{\sqrt{65}}{17} & 0 & \dfrac{3\sqrt{13}}{17} & 0 & \dfrac{30}{17} \end{pmatrix} \quad (A12)$$

For $K = 7$,

$$\tilde{B} = \begin{Bmatrix} \sqrt{2}\left(\dfrac{93}{256} + \dfrac{315z^2}{64} - \dfrac{3465z^4}{128} + \dfrac{3003z^6}{64} - \dfrac{6435z^8}{256}\right) \\[2mm] \sqrt{\dfrac{2}{3}}\left(\dfrac{-561z}{256} + \dfrac{3465z^3}{64} - \dfrac{27,027z^5}{128} + \dfrac{19,305z^7}{64} - \dfrac{36,465z^9}{256}\right) \\[2mm] \sqrt{\dfrac{2}{5}}\left(-\dfrac{495}{256} + \dfrac{1815z^2}{64} - \dfrac{17,325z^4}{128} + \dfrac{15,015z^6}{64} - \dfrac{32,175z^8}{256}\right) \\[2mm] \sqrt{\dfrac{2}{7}}\left(\dfrac{-3549z}{256} + \dfrac{8645z^3}{64} - \dfrac{63,063z^5}{128} + \dfrac{45,045z^7}{64} - \dfrac{85,085z^9}{256}\right) \\[2mm] \dfrac{\sqrt{2}}{3}\left(\dfrac{117}{256} + \dfrac{1755z^2}{64} - \dfrac{28,665z^4}{128} + \dfrac{27,027z^6}{64} - \dfrac{57,915z^8}{256}\right) \\[2mm] \sqrt{\dfrac{2}{11}}\left(\dfrac{-825z}{256} + \dfrac{9625z^3}{64} - \dfrac{93,555z^5}{128} + \dfrac{70,785z^7}{64} - \dfrac{133,705z^9}{256}\right) \\[2mm] \sqrt{\dfrac{2}{13}}\left(-\dfrac{975}{256} + \dfrac{6825z^2}{64} - \dfrac{61,425z^4}{128} + \dfrac{45,045z^6}{64} - \dfrac{83,655z^8}{256}\right) \\[2mm] \sqrt{\dfrac{2}{15}}\left(\dfrac{-8925z}{256} + \dfrac{26,775z^3}{64} - \dfrac{176,715z^5}{128} + \dfrac{109,395z^7}{64} - \dfrac{182,325z^9}{256}\right) \end{Bmatrix} \quad (A13)$$

$$P =
\begin{pmatrix}
\frac{18}{17} & 0 & \frac{\sqrt5}{17} & 0 & \frac{3}{17} & 0 & \frac{\sqrt{13}}{17} & 0 \\[4pt]
0 & \frac{22}{19} & 0 & \frac{\sqrt{21}}{19} & 0 & \frac{\sqrt{33}}{19} & 0 & \frac{3\sqrt5}{19} \\[4pt]
\frac{\sqrt5}{17} & 0 & \frac{22}{17} & 0 & \frac{3\sqrt5}{17} & 0 & \frac{\sqrt{65}}{17} & 0 \\[4pt]
0 & \frac{\sqrt{21}}{19} & 0 & \frac{26}{19} & 0 & \frac{\sqrt{77}}{19} & 0 & \frac{\sqrt{105}}{19} \\[4pt]
\frac{3}{17} & 0 & \frac{3\sqrt5}{17} & 0 & \frac{26}{17} & 0 & \frac{3\sqrt{13}}{17} & 0 \\[4pt]
0 & \frac{\sqrt{33}}{19} & 0 & \frac{\sqrt{77}}{19} & 0 & \frac{30}{19} & 0 & \frac{\sqrt{165}}{19} \\[4pt]
\frac{\sqrt{13}}{17} & 0 & \frac{\sqrt{65}}{17} & 0 & \frac{3\sqrt{13}}{17} & 0 & \frac{30}{17} & 0 \\[4pt]
0 & \frac{3\sqrt5}{19} & 0 & \frac{\sqrt{105}}{19} & 0 & \frac{\sqrt{165}}{19} & 0 & \frac{34}{19}
\end{pmatrix}
\tag{A14}$$

Acknowledgments

References

[1] Wang, J., and Yang, J., "Higher-Order Theories of Piezoelectric Plates and Applications," *Applied Mechanics Reviews*, Vol. 53, No. 1, 2000, pp. 87–99.

[2] Koiter, W. T., and Simmonds, J. G., "Foundations of Shell Theory," *Proceedings of the International Union of Theoretical and Applied Mechanics Congress*, Springer-Verlag, Berlin, 1972, pp. 150–176.

[3] Naghdi, P. M., "The Theory of Shells and Plates," *Handbuch der Physik*, Vol. 6a/2, edited by C. Truesdell, Springer-Verlag, Berlin, 1972, pp. 425–640.

[4] Antman, S. S., "The Theory of Rods," *Handbuch der Physik*, Vol. 6a/2, edited by C. Truesdell, Springer-Verlag, Berlin, 1972, pp. 641–703.

[5] Leissa, A. W., "Recent Research in Plate Vibrations, 1981–85, Part I: Classical Theory; *Shock and Vibration Digest*, Vol. 19, No. 2, 1987 pp. 11–18.

[6] Leissa, A. W., "Recent Research in Plate Vibrations, 1981–85, Part II: Complicating Effects," *Shock and Vibration Digest*, Vol. 19, No. 3, 1987, pp. 10–24.

[7] Cosserat, E., and Cosserat F., "Sur la Statique de la Ligne Deformable," *Comptes Rendus Hebdomadaires des Seances de l'Academie des Sciences*, Vol. 145, 1907, pp. 1409–1412.

[8] Teresi, L., and Tiero, A., "On Variational Approaches to Plate Models," *Meccanica*, Vol. 32, No. 2, 1997, pp. 143–156.

[9] Soldatos, K. P., and Watson, P., "Accurate Stress Analysis of Laminated Plates Combining Two-Dimensional Theory with the Exact Three-Dimensional Solution for Simply Supported Edges," *Mathematics and Mechanics of Solids*, Vol. 2, No. 4, 1997, pp. 459–489.

[10] Mindlin, R. C., and Medick, M. A., "Extensional Vibrations of Elastic Plates," *Journal of Applied Mechanics*, Vol. 26, No. 2, 1959, pp. 145–151.

[11] Vlasov, V. Z., "The Method of Initial Function in Problems of Theory of Thick Plates and Shells," *Proceedings of the 9th International Congress of Applied Mechanics*, Vol. 6, Universite de Bruxelles, Brussels, 1957, pp. 321–330.

[12] Lo, K. H., Christensen, R. M., and Wu, E. M., "A Higher-Order Theory of Plate Deformation, Part I: Homogeneous Plates," *Journal of Applied Mechanics*, Vol. 44, No. 4, 1977, pp. 669–676.

[13] Kant, T., "Numerical Analysis of Thick Plates," *Computational Methods in Applied Mechanics and Engineering*, Vol. 31, No. 1, 1982, pp. 1–18.

[14] Reddy, J. N., "A Simple Higher-Order Theory for Laminated Composite Plates," *Journal of Applied Mechanics*, Vol. 51, No. 4, 1984, pp. 745–752.

[15] Hanna, N. F., and Leissa, A. W., "A Higher Order Shear Deformation Theory for the Vibration of Thick Plates," *Journal of Sound and Vibration*, Vol. 170, No. 4, 1994, pp. 545–555.

[16] Lee, P. C.-Y., and Yu, J. D., "Governing Equations of Piezoelectric Plates with Graded Properties Across the Thickness," *IEEE Transactions on Ultrasonics, Ferroelectrics and Frequency Control*, Vol. 45, No. 1, 1998, pp. 236–250.

[17] Lee, P. C.-Y., Syngellakis, S., and Hou, J. P., "A Two Dimensional Theory for High-Frequency Vibrations of Piezoelectric Crystal Plates With or Without Electrodes," *Journal of Applied Mechanics*, Vol. 61, No. 4, 1987, pp. 1249–1262.

[18] Vidoli, S., and Batra, R. C., "Derivation of Plate and Rod Equations for a Piezoelectric Body from a Mixed Three-Dimensional Variational Principle," *Journal of Elasticity*, Vol. 59, Nos. 1–3, 2000, pp. 23–50.

[19] Yang, J. S., and Batra, R. C., "Mixed Variational Principles in Nonlinear Piezoelectricity," *International Journal of Nonlinear Mechanics*, Vol. 30, No. 5, 1995, pp. 719–726.

[20] Vel, S. S., and Batra, R. C., "Cylindrical Bending of Laminated Plates with Distributed and Segmented Piezoelectric Actuators/Sensors," *AIAA Journal*, Vol. 38, No. 5, 2000, pp. 857–867.

[21] Batra, R. C., Vidoli, S., and Vestroni, F., "Plane Wave Solutions and Modal Analysis in Higher-Order Shear and Normal Deformable Plate Theories," *Journal of Sound and Vibration* (submitted for publication).

[22] Vel, S. S., and Batra, R. C., "The Generalized Plane Strain Deformations of Thick Anisotropic Composite Laminated Plates," *International Journal of Solids and Structures*, Vol. 37, No. 5, 2000, pp. 715–733.

A. M. Waas
Associate Editor